AGU PUBLICATIONS

Tectonics

RESEARCH ARTICLE
10.1002/2014TC003539

Key Points:
- The Rehamna metamorphic dome (Moroccan Variscan belt) suffered a tectonic switch
- It is bracketed at the Carboniferous-Permian boundary ($^{40}Ar/^{39}Ar$ geochronology)
- It reflects change in plate configuration during Alleghanian-Variscan orogeny

Supporting Information:
- Readme
- Table S1
- Table S2
- Table S3
- Table S4
- Table S5
- Table S6
- Table S7
- Table S8
- Table S9
- Table S10
- Table S11
- Table S12

Correspondence to:
F. Chopin,
chop1fran6@gmail.com

Citation:
Chopin, F., M. Corsini, K. Schulmann, M. El Houicha, J.-F. Ghienne, and J.-B. Edel (2014), Tectonic evolution of the Rehamna metamorphic dome (Morocco) in the context of the Alleghanian-Variscan orogeny, *Tectonics*, *33*, 1154–1177, doi:10.1002/2014TC003539.

Received 24 JAN 2014
Accepted 9 MAY 2014
Accepted article online 22 MAY 2014
Published online 18 JUN 2014

Tectonic evolution of the Rehamna metamorphic dome (Morocco) in the context of the Alleghanian-Variscan orogeny

Francis Chopin[1,2,3,4], Michel Corsini[2], Karel Schulmann[1,3], Mohamed El Houicha[5], Jean-François Ghienne[3], and Jean-Bernard Edel[3]

[1]Centre for Lithospheric Research, Czech Geological Survey, Prague, Czech Republic, [2]Geoazur, CNRS UMR6526—Université Nice Sophia Antipolis, Valbonne, France, [3]Institut de Physique du Globe de Strasbourg, UMR7516 CNRS—Université de Strasbourg, École et Observatoire des Sciences de la Terre, Strasbourg, France, [4]Department of Geosciences and Geography, University of Helsinki, Helsinki, Finland, [5]Département de Géologie, Faculté des Sciences, Université Chouaïb Doukkali, El Jadida, Morocco

Abstract Structural and $^{40}Ar/^{39}Ar$ geochronological investigations of the Rehamna Massif (Meseta, Moroccan Variscan belt) provide new constraints on the tectonic evolution of the Alleghanian-Variscan orogen during the Upper Paleozoic. Three main tectonic events have been recognized: (1) Southward thrusting of an Ordovician sequence over the Proterozoic basement, its Cambrian sedimentary cover, and the overlying Devono-Carboniferous basin. This event caused subhorizontal shearing and prograde Barrovian metamorphism of the buried rocks. (2) Continuous shortening resulting in the development of a synconvergent extrusion of metamorphosed units to form a dome elongated E-W. This was responsible for synconvergent detachment of the Ordovician upper crustal sequence. The timing of these two episodes is constrained to 310–295 Ma by cooling and metamorphic amphibole and mica ages (3) A NW-WNW convergence in a direction orthogonal to the previous one and characterized by the accretion of the Rehamna dome to the continental basement in the east. Based on $^{40}Ar/^{39}Ar$ cooling ages from a syntectonic granitoid and its host rocks and metamorphic $^{40}Ar/^{39}Ar$ ages from greenschist facies mylonite, the timing of this event falls between 295 and 280 Ma. The end of the Variscan orogeny in the Moroccan Meseta is constrained by the $^{40}Ar/^{39}Ar$ cooling age of a posttectonic pluton dated at ~275 Ma. The tectonic events highlighted in Morocco coincide with the late Variscan-Alleghanian tectonic evolution of southern Europe and North America and can be correlated with the global reorganization of plates that accompanied suturing of Pangaea at around 295 Ma.

1. Introduction

New structural and geochronological information about the Rehamna Massif (western Morocco) is presented in this paper and placed in the framework of a consistent model for the Alleghanian-Variscan orogeny. Until now, the scarcity of combined structural and geochronological studies from the Moroccan Variscan belt [*Gasquet*, 1996; *Essaifi et al*., 2003; *Tahiri et al*., 2010] prevented better understanding of the tectonic evolution of this branch of the Variscan orogen and correlations with adjacent areas in the European Variscan belt and the Alleghanian-Appalachian orogen [e.g., *Michard et al*., 2010b]. Recent structural studies of the Alleghanian belt on the eastern seaboard of the United States [*Hatcher*, 2002, 2010; *Engelder and Whitaker*, 2006] and in Iberia [*Gutiérrez-Alonso et al*., 2011, 2012] have highlighted the complexity of tectonic evolution during the Upper Carboniferous-Lower Permian orogeny caused by changes in the orientation of the principal tectonic stresses during the Upper Carboniferous. In the Moroccan Meseta, the main Variscan deformation is considered to be related to dextral transpression along the Western Meseta Shear Zone (WMSZ) of *Piqué et al*. [1980] during the Middle to Upper Paleozoic (Figure 1). This interpretation is commonly used in geodynamic models that involve the amalgamation of Laurussia with Gondwana and derived fragments to form the Alleghanian-Variscan belt [e.g., *Matte*, 2001; *Hœpffner et al*., 2005; *Simancas et al*., 2009; *Michard et al*., 2010b].

The subject of the present paper is a key unit of the Moroccan belt, known as the Rehamna Massif. Based on a large structural and $^{40}Ar/^{39}Ar$ geochronological data set, the regional tectonic evolution of this unit is interpreted and placed in the context of the orogen as a whole. The results of this study challenge the concepts of long-lived Variscan dextral shearing along the NW Gondwana margin, and a new two-stage tectonic model that complements earlier geodynamic scenarios is proposed for the Alleghanian-Variscan

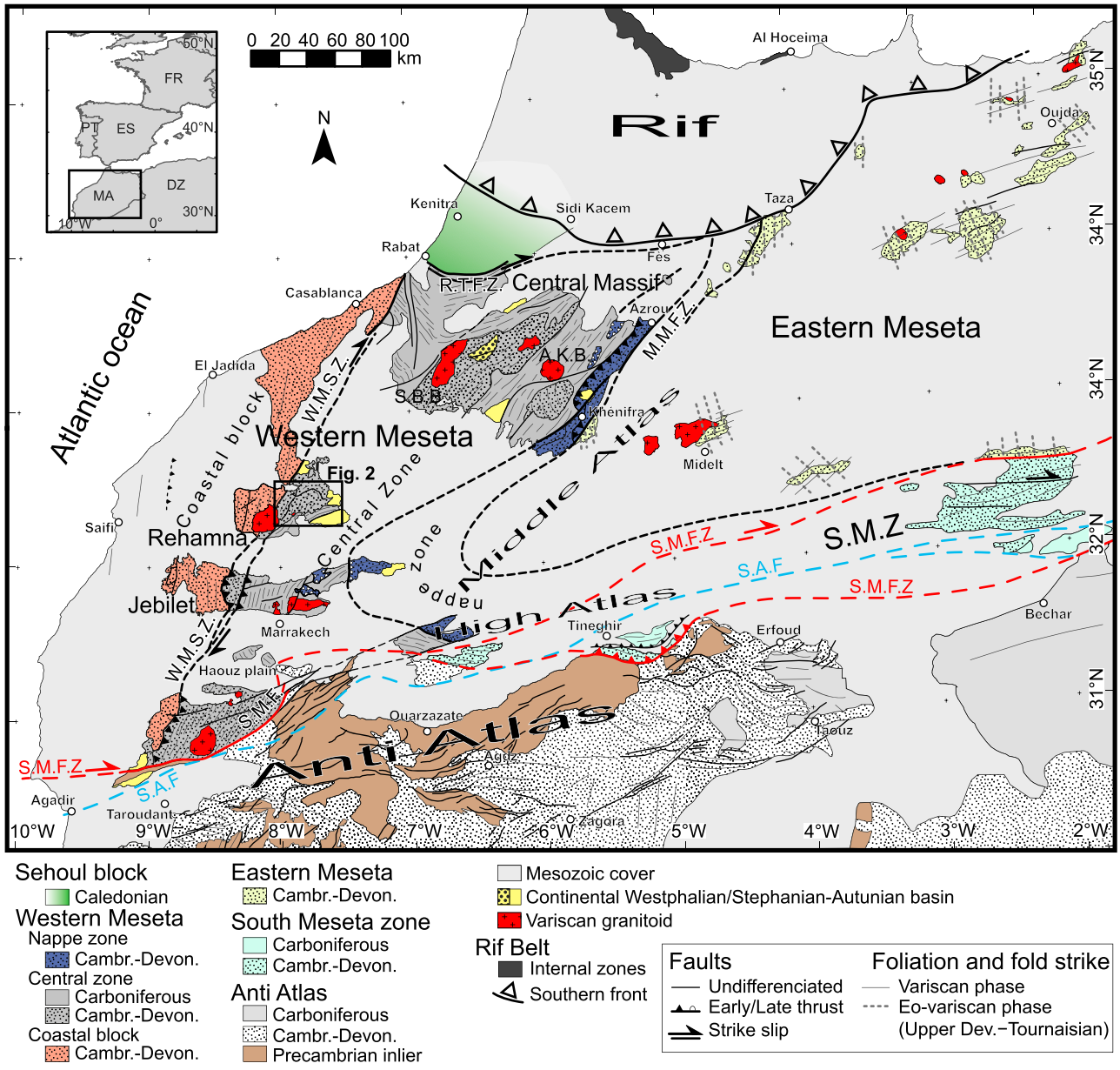

Figure 1. Simplified geological map of the MoroccanVariscides (modified after *Hœpffner et al.* [2005], *Michard et al.* [2008], and *Michard et al.* [2010a]). Middle Meseta Fault Zone (MMFZ), Western Meseta Shear Zone (WMSZ), South Meseta Fault Zone (SMFZ), South Atlas Fault (SAF), Rabat-Tiflet Fault Zone (RTFZ), Sidi Bettache basin (SBB), and Azrou Khenifra basin (AKB).

orogeny [*Hatcher*, 2002, 2010; *Engelder and Whitaker*, 2006; *Gutiérrez-Alonso et al.*, 2011, 2012]. This new approach highlights the importance of earlier N-S compressive deformation related to the convergence between Gondwana and the European Variscan belt during the Upper Carboniferous, followed by frontal E-W collision between Gondwana and Laurentia during the Lower Permian.

2. Geological Setting

2.1. The Moroccan Variscides

The Moroccan Variscan belt (Figure 1) is considered to be the southwestern continuation of the European Carboniferous orogen on the NW Gondwana margin. It can be divided into five main tectonic zones [e.g., *Hœpffner et al.*, 2005, 2006b; *El Hadi et al.*, 2006; *Simancas et al.*, 2009; *Michard et al.*, 2008, 2010a]: (1) the Anti-Atlas

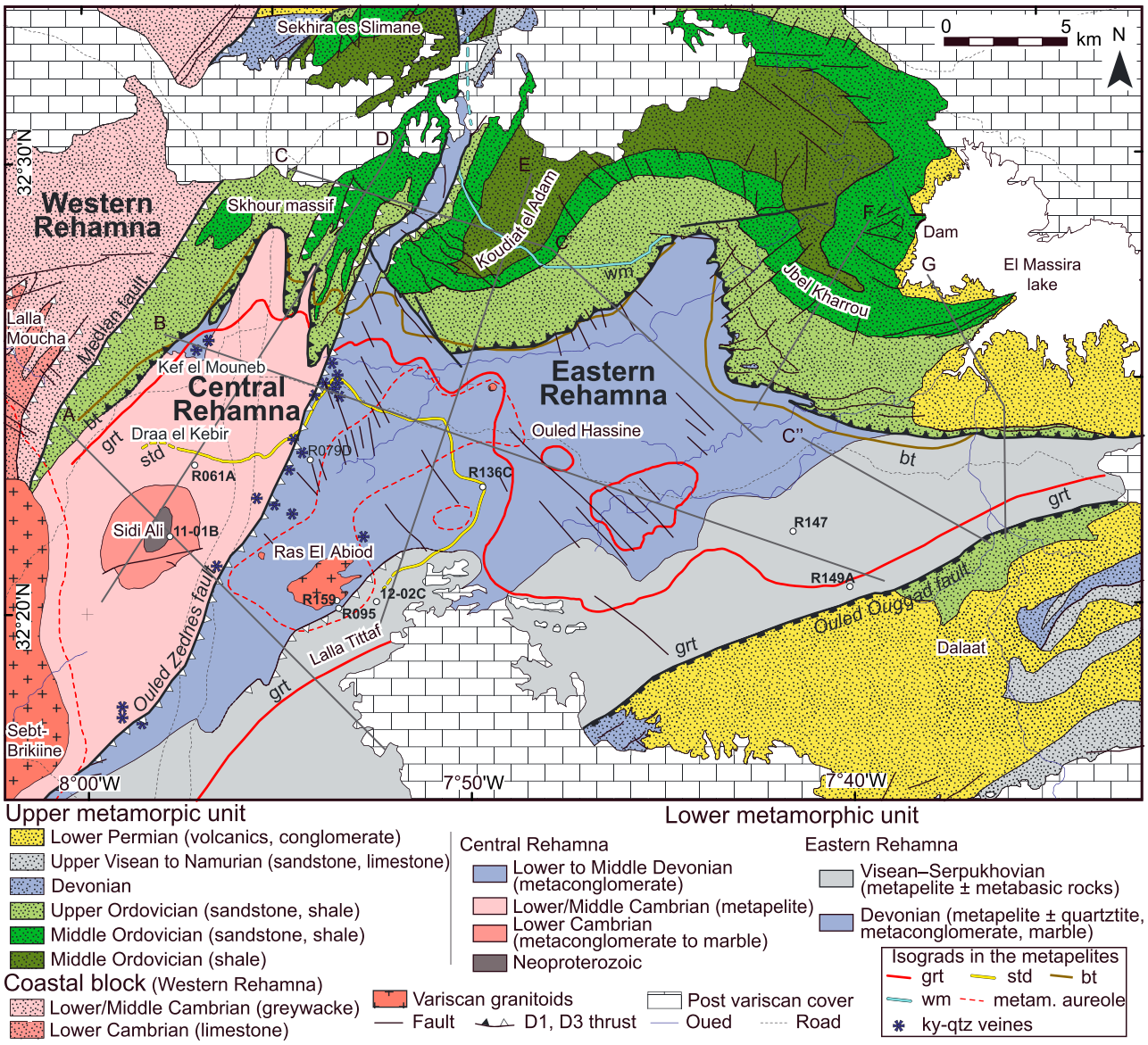

Figure 2. Lithological map of the Rehamna Massif (modified after *Hœpffner et al.* [1975b], *Michard* [1982], *Cornée* [1982], *Corsini* [1988], *Corsini et al.* [1988b], *Baudin et al.* [2003], *Razin et al.* [2003], *El Kamel and El Hassani* [2006], and *Michard et al.* [2010b]) showing the locations of samples used for geochronology. Grt and Bt isograds modified after *Michard* [1982], *Cornée and Muller* [1981], *Cornée* [1982], *Baudin et al.*[2003], and *Razin et al.* [2003]; Std isograd modified after *Hœpffner et al.* [1982] and *Aghzer and Arenas* [1995].

to the south belongs to the thick-skinned Variscan foreland (Figure 1) composed of inverted Lower to Middle Paleozoic sediments of the Gondwana passive margin within which the intensity of deformation decreases toward the continent in the south [e.g., *Burkhard et al.*, 2006]. (2) The Western Meseta consists of the western Coastal Block, the Central Zone, and the Nappe Zone in the east. It is a vast region affected by widespread orogenic, generally peraluminous, felsic magmatism [*Mrini et al.*, 1992; *Gasquet et al.*, 1996]. The Coastal Block consists of Cambrian to Devonian sediments covering Proterozoic basement (Figure 1) and shows only weak deformation [*Hœpffner et al.*, 2005, and references therein] increasing toward the Western Meseta Shear Zone (WMSZ) [*Piqué et al.*, 1980]. The Central Zone is formed by Devono-Carboniferous intracontinental basins and underlying Proterozoic basement (Figure 1). These basins are intensively reworked by late Paleozoic deformation that took place in a relatively high Barrovian geothermal gradient [*Aghzer and Arenas*, 1998; *Michard et al.*, 2010b]. This Variscan metamorphic zone crops out in three separated crystalline massifs which are from the north to the south: the Central

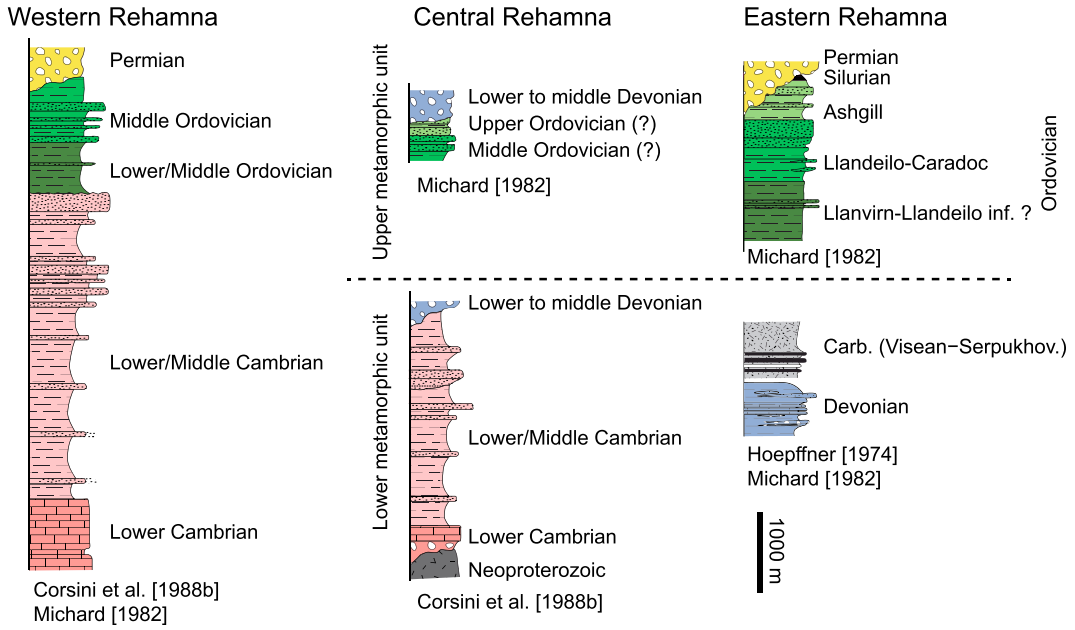

Figure 3. Synthetic lithostratigraphic logs of the Rehamna Massif subdivided into the Western (i.e., Coastal Block), Central, and Eastern Rehamna, and the orogenic suprastructure and infrastructure (modified after *Michard* [1982], *Hœpffner* [1974], and *Corsini et al.* [1988b]).

Massif, Rehamna, and Jebilet. (3) The Eastern Meseta (Figure 1) is made up of small Paleozoic massifs affected by Upper Devonian-Tournaisian (i.e., Eo-Variscan) deformation [*Marhoumi et al.*, 1983]. This is separated from the Western Meseta by the Middle Meseta Fault Zone (MMFZ), whereas the South Meseta Zone (SMZ) (4) is a transitional domain separating the Meseta and Anti-Atlas zones [*Michard et al.*, 2010a]. (5) The Sehoul block in the North (Figure 1) was accreted to the whole Meseta domain along the Rabat-Tiflet Fault Zone (RTFZ) during the Upper Devonian-Lower Carboniferous [*Tahiri et al.*, 2010; *Michard et al.*, 2010b].

This general structure results from the reorganization of the NW Gondwana margin during closure of the Rheic Ocean from the Devonian to the Upper Carboniferous. There are two tectonic models that are used to explain the formation of the Moroccan Variscan belt: 1. In the most popular model, a polyphase evolution of the belt is proposed starting with westward convergence in the Eo-Variscan (i.e., Upper Devonian-Tournaisian) that affected the Eastern Meseta. This event is associated with the formation of NNE striking transtensional basins in the Central Zone, followed by westward transpressional accretion of this zone to the Coastal Block during the Upper Carboniferous accompanied by N-S shortening of the Eastern Meseta [*Hœpffner*, 1987; *Bouabdelli and Piqué*, 1996; *Hœpffner et al.*, 2005, 2006a, 2006b; *Michard et al.*, 2010a]. This important late deformation results in the E-W structural grain of the Eastern Meseta and the NNE structural grain of the Western Meseta. According to this scheme, the Rheic suture separating the Gondwana and Laurentia continents is hidden in the present Atlantic passive margin and continues into the African continent as the Rabat-Tiflet Fault Zone [*Hœpffner et al.*, 2005, 2006b; *Michard et al.*, 2010b; *Tahiri et al.*, 2010]. 2. The alternative model proposes a continuous compression of the Variscan foreland to form the whole Moroccan Meseta in which the Rheic suture is hidden at the eastern boundary of the Eastern Meseta [*Kharbouch et al.*, 1985, *Boulin et al.*, 1988; *Roddaz et al.*, 2002, 2006; *Essaifi et al.*, 2014]. In both models, large-scale deformation is accommodated by strike-slip movement along the South Meseta Fault Zone and the Rabat-Tiflet Fault Zone [*Michard et al.*, 2010a, 2010b, and references therein].

2.2. The Geology of the Rehamna Massif

The Rehamna Massif is located in the Western Meseta (Figures 1 and 2). It is divided into three main structural units separated by the Median (part of the WMSZ) and the Ouled Zednes faults [*Michard et al.*,

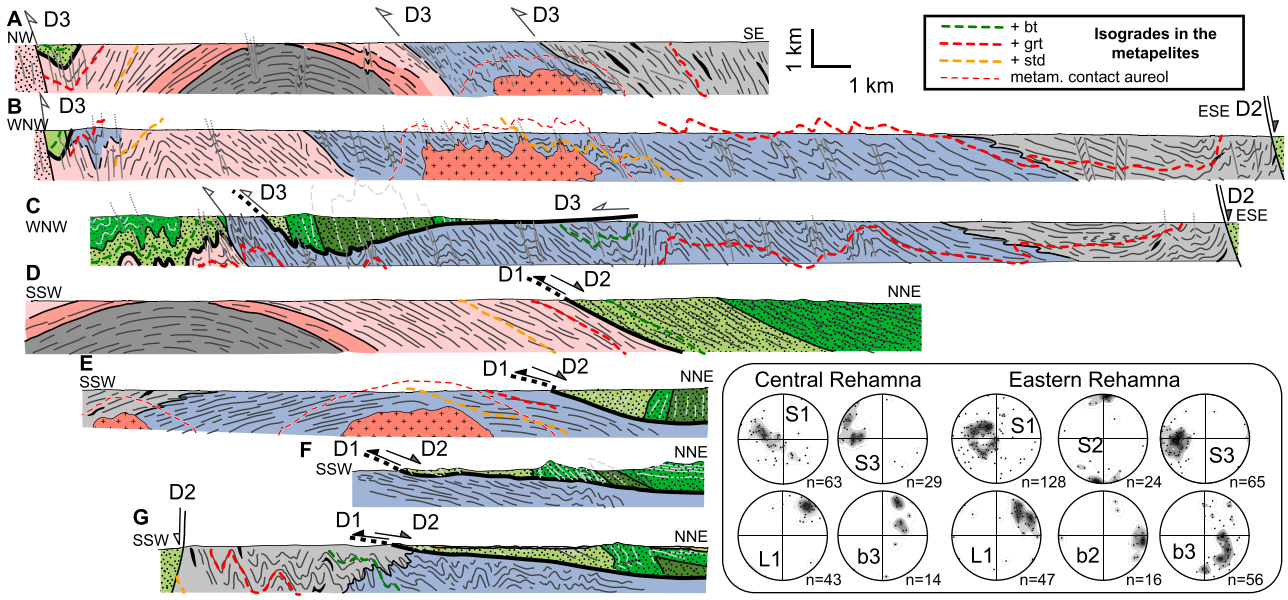

Figure 4. Interpretative geological cross sections through the Rehamna Massif. Stereographic diagrams show equal area, lower hemisphere projections of planar and linear structures.

2010b, and references therein]. These are the Western Rehamna, which belongs to the Coastal Block, and the Central and Eastern Rehamna of the Central Zone (Figure 2). Based on the intensity of deformation and the degree of metamorphism, the Rehamna Massif was subdivided into upper and lower metamorphic units by *Baudin et al.* [2003] and *Razin et al.* [2003].

The lithostratigraphy of the Rehamna Massif is shown in simplified stratigraphic columns in Figure 3. The Western Rehamna (Figure 2) includes Lower-Middle Cambrian to Ordovician anchizonal succession, which is made up of basal Lower Cambrian limestones and siliciclastic sediments [*Michard*, 1967; *Guézou and Michard*, 1976; *Destombes et al.*, 1982; *Bernardin et al.*, 1988; *Corsini et al.*, 1988b]. In the metamorphosed Central Rehamna (lower metamorphic unit), equivalent metasedimentary rocks lie on a Neoproterozoic metarhyolitic basement (Sidi Ali dome, [*Corsini et al.*, 1988b]) and terminates with Lower-Middle Devonian metaconglomerates (Kef el Mouneb formation, [*Destombes et al.*, 1982]) with tectonic [*Corsini et al.*, 1988a; *Diot*, 1989; *Baudin et al.*, 2003] or sedimentary unconformity [*Hœpffner et al.*, 1975b; *Michard et al.*, 2010b]. In contrast, *Aghzer and Arenas* [1995] interpret the Kef El Mouneb formation as a tectonic window. The age of the upper metamorphic unit sediments (pelite and sandstone) in the Skhour area is more controversial [*Baudin et al.*, 2003], and they are attributed either to the Cambro-Ordovician [*Hœpffner et al.*, 1975a, 1975b; *Destombes et al.*, 1982] or to the Upper Devonian [*Michard*, 1969; *Michard et al.*, 2010b] in a discordant or concordant setting, respectively (Figure 3). In the Eastern Rehamna, the Devonian Ouled Hassine (pelite ± quartzite, conglomerate and marble) and supposedly Lower Carboniferous (Visean-Serpukhovian) Lalla Tittaf (pelite ± amphibolite and metarhyolite) metasedimentary formations [*Destombes et al.*, 1982; *Cornée et al.*, 1982, *Michard et al.*, 2010b] are attributed to the lower metamorphic unit (Figure 3). To the north, the very low-grade upper metamorphic unit rocks of the Koudiat El Adam and Jbel Kharrou areas are mainly Middle Ordovician to Silurian shale and sandstone [*Destombes et al.*, 1982], whereas Devonian (sandstone and mudstone) and Visean (sandstone and limestone) sediments also crop out in the southern Dalaat area [*Cornée*, 1982; *Destombes et al.*, 1982; *Rais-Assa et al.*, 1983]. These rocks are covered by volcanics and molassic conglomerates of Upper Westphalian to supposedly Autunian age [*Hœpffner et al.*, 1975b; *Destombes et al.*, 1982].

The structure of the Rehamna Massif has been interpreted to be the result of (1) dextral transpression against the Western Rehamna-Coastal Block [*Piqué et al.*, 1980] resulting from the increasing intensity of folding and shearing in the Central Rehamna rocks and (2) (north) westward thrusting of the Eastern Rehamna over the Central Rehamna rocks further east [*Hœpffner et al.*, 1975a, 1975b; *Piqué et al.*, 1982; *Lagarde and Michard*, 1986; *Lagarde et al.*, 1990; *Diot and Bouchez*, 1991]. Nevertheless, *Corsini et al.* [1988a] and *Diot* [1989]

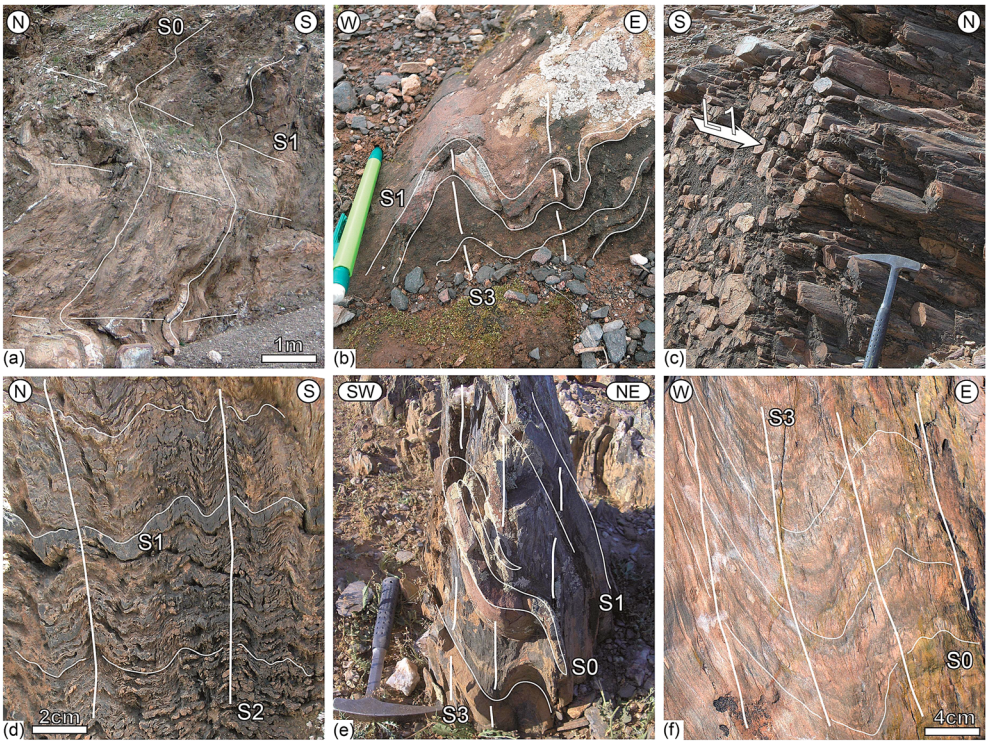

Figure 5. Field photographs showing deformation structures in the Rehamna Massif. (a) Recumbent open F1 folds in Middle Ordovician sandstones and shales from the upper metamorphic unit (Jbel Kharrou). (b) Upright close asymmetric NNE-SSW striking F3 folds folding S1 metamorphic foliation in Lower Cambrian marble from the lower metamorphic unit (Sidi Ali). (c) Strongly prolate NNE-SSW striking L1 fabric in Devonian conglomerates from Kef El Mouned in the lower metamorphic unit. (d) E-W striking upright close F2 folds folding S1 metamorphic foliation in metapelites from the eastern-most part of the Carboniferous Lalla Tittaf formation of the lower metamorphic unit. (e) Upright open asymmetric NE-SW striking F3 folds with relics of bedding S0 and metamorphic foliation S1 in quartzite and metapelites from the Devonian Ouled Hassine formation of the lower metamorphic unit. (f) Upright close asymmetric NNE-SSW striking F3 folds in Upper Ordovician shales from the Skhour area of the upper metamorphic unit. Number in the bottom left.

questioned the role of the transpressional regime and highlighted the importance of early orogen-parallel flow. The general domal structure [*Corsini et al.*,1988a] of the whole Rehamna Massif has been interpreted as a result of late orogenic extensional collapse [*Aghzer and Arenas*, 1995; *El Mahi et al.*, 2000a; *Baudin et al.*, 2003; *Razin et al.*, 2003; *Michard et al.*, 2010b].

Two main metamorphic events have been described in the Rehamna. The first one is a syntectonic metamorphism affecting the lower metamorphic unit and reaching the staurolite stability field at around 6–9 kbar and 410–560°C [*Diot*, 1989; *Aghzer and Arenas*, 1995, 1998; *El Mahi et al.*, 2000a]. This is followed by a syntectonic to late tectonic metamorphism penecontemporaneous with the intrusion of the Ras El Abiod and Sebt-Brikiine granitoids, respectively [*Hœpffner et al.*, 1982; *Diot and Bouchez*, 1991; *Lagarde et al.*, 1990; *Baudin et al.*, 2003]. Metamorphic isograds and aureoles [*Michard et al.*, 2010b, and references therein] for both events are shown in Figure 2.

A limited number of age determinations have been made on the Rehamna granitoids. U-Pb zircon dating of a microgranite porphyric dyke close to the syntectonic Ras El Abiod leucogranite yielded an age of 285.4 ± 6.1 Ma [*Baudin et al.*, 2003]. *Mrini et al.* [1992] obtained a younger age of 268 ± 6 Ma (Rb-Sr) for the late tectonic Sebt-Brikiine granite and an age of ~265 Ma for related dykes. This is comparable to the age of 278 ± 2 Ma (Rb − Sr) recalculated by *Hœpffner et al.* [1982] based on the work of *Tisserant* [1977] in the same complex. Despite preliminary Rb-Sr work by the latter author, no dates for metamorphic rocks are available. Therefore, Variscan orogenic deformation is considered to have taken place after the deposition of the Lalla Tittaf formation of supposed Visean-Serpukhovian age (see discussion in *Michard et al.* [2010b]) and before the intrusion of the late-tectonic Sebt-Brikiine granite of Permian age.

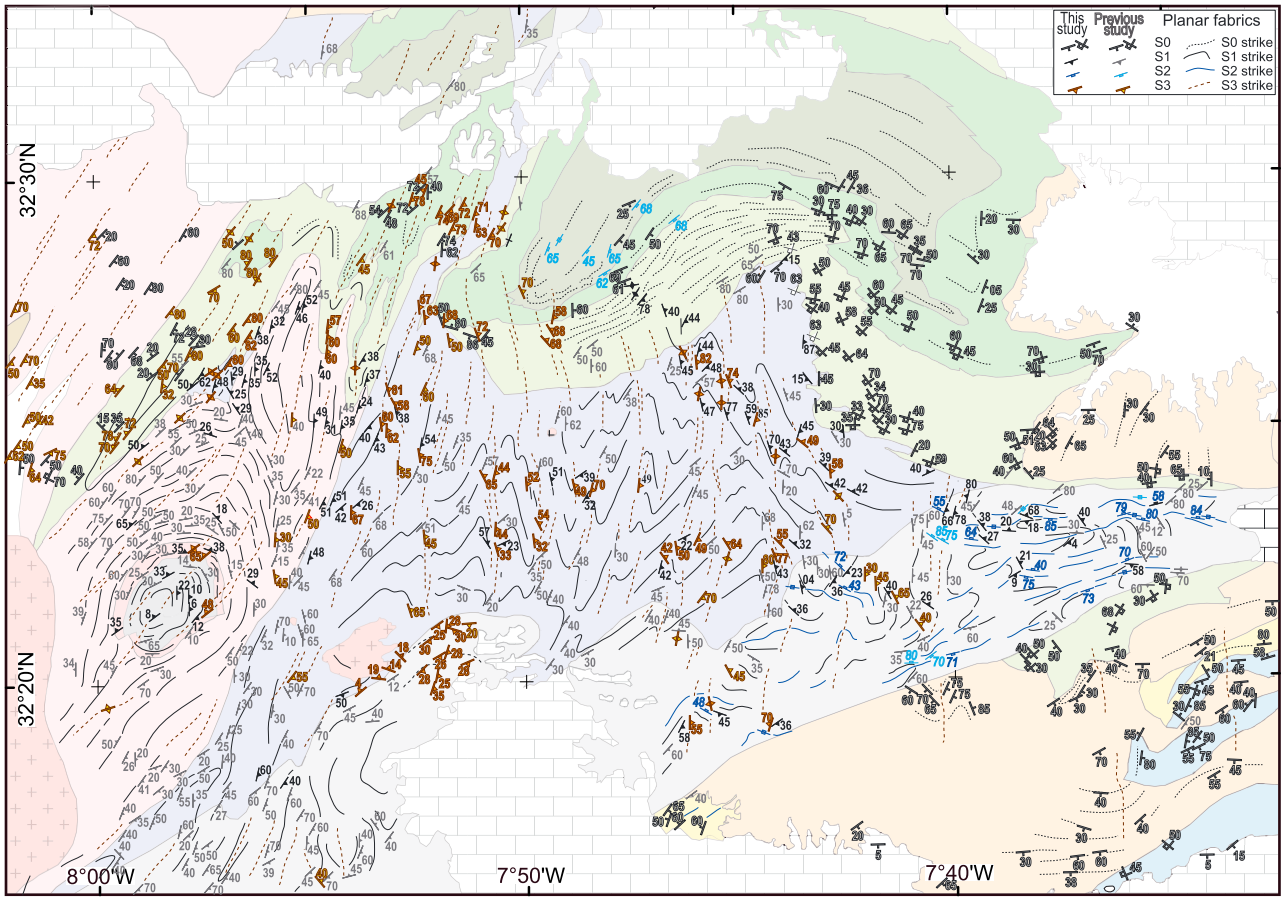

Figure 6. Structural map of planar structures in the Rehamna showing the distribution and relationships between planar fabrics with data from this study and from *Hœpffner* [1974], *Cornée* [1982], *Lagarde and Michard* [1986], *Corsini* [1988], *Corsini et al.* [1988a], *Diot* [1989], *Aghzer and Arenas* [1995], *Baudin et al.* [2003], and *Razin et al.* [2003].

3. Structural Evolution

Three main deformation events (D1, D2, and D3) of variable intensity and geometry were identified in the Rehamna Massif. The first one forms the initially flat-lying metamorphic foliation S1 which is deformed by F2 folds trending WSW-ENE with associated subvertical S2 cleavage and is then heterogeneously reworked by F3 folds trending NNE-SSW with an S3 cleavage dipping moderately to steeply ESE.

3.1. D1 and D2 Structures

The preservation of D1 structures across the whole Rehamna Massif is variable. In the Ordovician sequences of the upper metamorphic unit, SSW directed movement is expressed by the formation of a fold-and-thrust belt structural pattern, as shown in the map and cross section (Figures 2 and 4d–4g). Here the D1 deformation is manifested mainly by the kilometer-scale overturned Koudiat el Adam-Jbel Kharrou anticline with a core of Lower-Middle Ordovician shales. Meter-scale recumbent F1 folds affect the Ordovician beds (Figure 5a), sometimes with associated development of the S1 slaty cleavage. The asymmetry of the recumbent folds indicates southward thrusting as shown by the shape of the large-scale Koudiat el Adam-Jbel Kharrou anticline.

In the lower metamorphic unit, the D1 structures are characterized by an early penetrative S1 schistosity affecting the Neoproterozoic basement and its Paleozoic sedimentary cover (Figures 5b). This fabric is well preserved in the Central Rehamna where it forms a shallowly to moderately dipping S1 foliation (Figure 6) bearing a strong NNE-SSW lineation (Figures 5c and 7). Kinematic criteria such as the preferred crystallographic orientation of quartz [*Diot*, 1989], C/S structures, and σ winged (porphyro-) clasts [*Corsini et al.*, 1988a; *Diot*, 1989] indicate a top to the S-SSW shearing associated with this event.

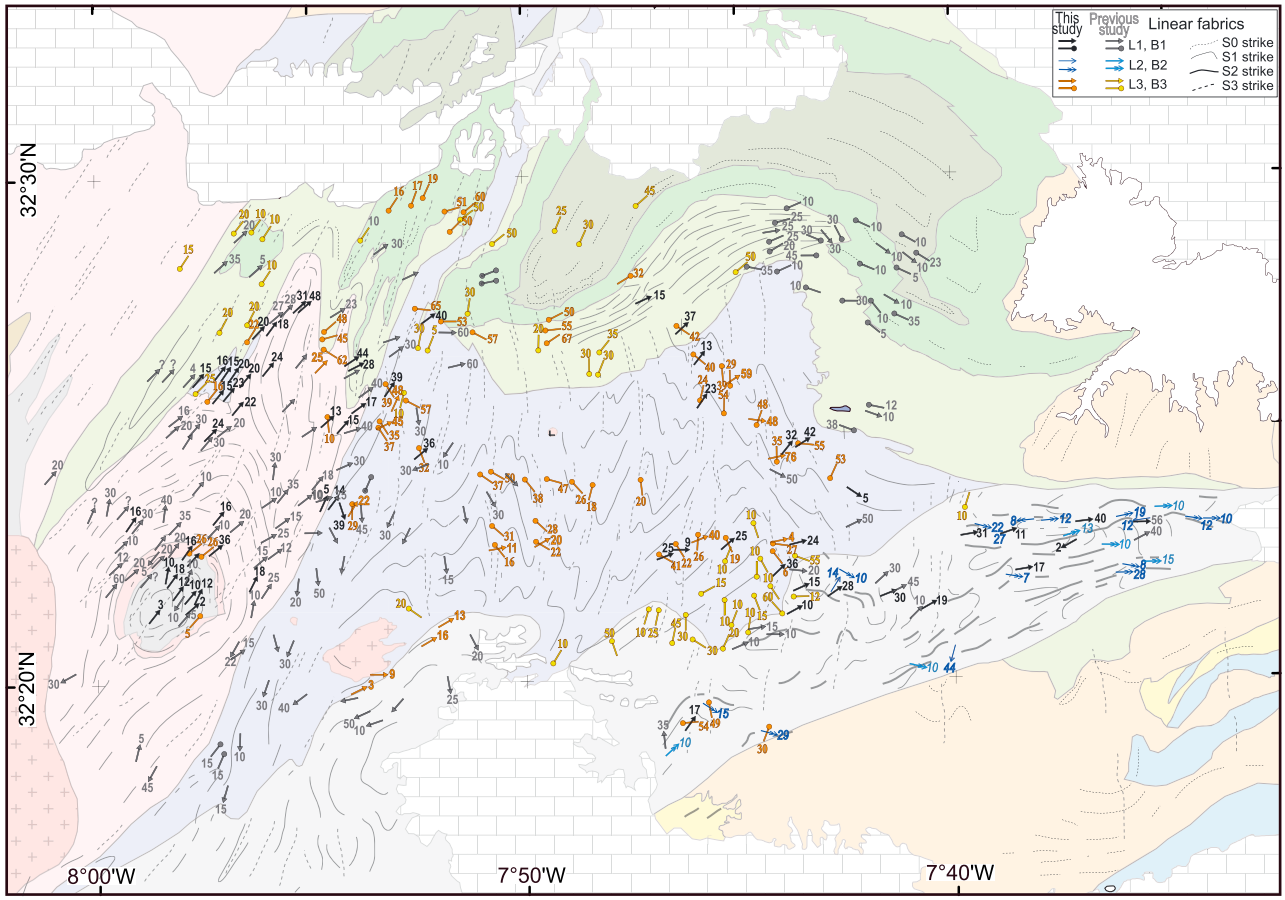

Figure 7. Structural map of linear structures with the trend of planar structures from Figure 6 including data from this study and from *Hœpffner* [1974], *Cornée* [1982], *Lagarde and Michard* [1986], *Corsini* [1988], *Corsini et al.* [1988a], *Diot* [1989], *Aghzer and Arenas* [1995], *Baudin et al.* [2003], and *Razin et al.* [2003].

In the Eastern Rehamna, the S1 metamorphic foliation does not bear a strong lineation, but consistent asymmetrical criteria indicating the sense of shear were also observed. Here the S1 schistosity is affected by ~W-E upright F2 chevron folds (Figures 4g, 5d, and 6) with subhorizontal fold axes (Figure 7) associated with development of an S2 axial planar cleavage and locally complete transposition of S1 into a composite S1-S2 foliation. In less deformed areas, conjugate F2 kink bands with E-W oriented hinge zones affect the S1 foliation. Further west, the intensity of D2 shortening decreases and the S1 fabric is folded into a WSW-ENE trending upright kilometer-scale open to tight F2 antiform (Figures 4d and 4e).

3.2. D3 Structures

The D3 deformation caused heterogeneous reworking of the whole Rehamna Massif that was locally intense. In the eastern part of the Eastern Rehamna the intensity of D3 deformation is weak and takes the form of heterogeneously developed kink bands with NNE-SSW oriented hinge zones. Going to the west, the S1-S2 foliation is progressively more affected by decimeter- to meter-scale, tight to isoclinal, overturned NNE-SSW striking folds with moderately to steeply dipping axial planes and gently to steeply dipping fold axes. The stereographic projection of F3 fold axes for the Eastern Rehamna shows a girdle distribution with a wide E-ESE central maximum (Figure 4). This pattern of F3 axial directions reflects the E-W orientation of S2 schistosity dipping variably to the north or south which has been refolded by upright F3 folds (Figure 6). Increase in the intensity of folding is associated with the formation of a new S3 axial plane cleavage (Figure 5e) dipping steeply E to ESE (Figures 4a–4c). Close to the Ouled Zednes Fault, the cleavage gradually transforms to an S3 mylonitic foliation related to the thrusting of the Eastern Rehamna over the Central Rehamna (Figure 2) [*Lagarde and Michard*, 1986; *Aghzer and Arenas*, 1995].

South of the Ras El Abiod granite, the composite S1-2 WSW-ENE trending vertical schistosity is affected by D3 event (Figure 6). Here S3 takes the form of a moderately to gently dipping axial plane cleavage in recumbent WSW-ENE trending F3 folds (Figure 4a). The concentration of D3 deformation in this area was interpreted by *Cornée et al*. [1982] to be the result of reactivation of the boundary between the Carboniferous Lalla Tittaf and Devonian Ouled Hassine basins (Figure 2).

In the Central Rehamna, the D3 deformation is expressed by large-scale folding of the S1 fabric in a kilometer-scale SSW-NNE anticline in which the hinge zone is coinciding with the circular outcrop of the Neoproterozoic basement (Figures 4a–4c and 6, Sidi Ali area). The basement forms an almost symmetrical dome structure which results from interference between WSW-ENE oriented F2 and NNE-SSW oriented F3 upright anticlines of similar wavelength. The S3 cleavage is only rarely developed in small asymmetric F3 folds (Figure 5b). Close to the Median fault (WMSZ), the horizontal WNW-ESE directed D3 shortening causes reworking of stretched quartz pebbles with long axes parallel to the NNE-SSW oriented L1 stretching direction. This superposition of strain results in extreme elongation of quartz pebbles in a NNE-SSW direction and the formation of a prolate fabric in this area (Figure 5c, Kef El Mouneb).

The D3 event also heterogeneously affects the Ordovician sequences (upper metamorphic unit) in the north of the studied area. In the Eastern Rehamna, it is responsible (Figure 2) for kilometer-scale refolding of the D1 thrust and fold belt structure by an upright F3 anticline with a hinge plunging moderately to the north. As a consequence, the fold hinge of the Koudiat el Adam-Jbel Kharrou anticline is rotated to a NE-SW direction on the western flank and to a NW-SE direction on the eastern flank of this regional-scale F3 anticline (Figures 4 and 6). The intensity of F3 folding increases toward the Ouled Zednes Fault Zone so that the western part of the Koudiat el Adam-Jbel Kharrou anticline is thrust to the WNW over the tightly attenuated Devonian rocks of Central Rehamna (Figure 4c) [*Michard*, 1982]. F3 folds are also well developed at the outcrop scale in the southern termination of the Koudiat el Adam anticline. Here quartzite layers and underlying Devonian pelites are refolded together by open to close upright folds with fold axes plunging moderately to the NE (Figure 7). In the Skhour and Sekhira-es-Slimane areas of the Central Rehamna (Figure 2), the bedding of Cambro-Ordovician sandstones is folded by close to tight upright folds with hinges plunging gently to the NE. These folds are associated with a disjunctive S3 fracture cleavage dipping steeply east (Figures 5f and 6) and northwestward imbrication of the Ordovician sequences (Figures 4c and 6) [*Michard*, 1982].

The style of D3 deformation is similar in the Western Rehamna (i.e., Coastal Block), where the open to close upright F3 folds are commonly associated with a subvertical cleavage and imbrication of the Cambrian sequences (Figures 4a, 4b, and 6). This folding is particularly well developed in the Lalla Moucha area where kilometer-scale F3 folds occur (Figure 2). As reported by previous investigators, the intensity of D3 deformation decreases progressively toward the west within the Coastal Block [*Guézou and Michard*, 1976; *Corsini et al*., 1988a].

4. Links Between Deformation, Metamorphism, and the Intrusion of Granitoids

Even though the metamorphic evolution of the Rehamna Massif has been studied by numerous authors [e.g., *Hœpffner et al*., 1982; *Corsini et al*., 1988a; *Diot*, 1989; *Aghzer and Arenas*, 1998], the relationship between deformation and metamorphism across the whole massif has not been considered in detail. The study of oriented thin sections shows that the first metamorphic foliation S1 developed in a relatively HT Barrovian gradient reaching the Grt-St stability field in the center of the massif. This fabric was formed throughout the whole lower metamorphic unit, from the Neoproterozoic basement and its cover in the Central Rehamna (Figures 8a−8c) to the Devonian Ouled Hassine (Figures 8d and 8e) and Carboniferous Lalla Tittaf (Figures 8g–8i) formations of the Eastern Rehamna. Compositional layering S0 is sometimes well preserved in weakly metamorphosed metasediments (Figures 8b and 8i). Biotite, garnet, and staurolite progressively grow in the prograde gradient as shown by textural relationships (e.g., garnet enclosed in staurolite porphyroblasts, Figure 8c) and by the normal zonation of garnet porphyroblasts [*Aghzer and Arenas*, 1995, 1998; *El Mahi et al*., 2000a].

In the Eastern Rehamna, the S2 cleavage affects the S1 metamorphic foliation forming chevron microstructures (Figure 8i) around garnet porphyroclasts, which retain subhorizontal primary inclusions, whereas chlorite grows in surrounding pressure shadows (Figure 8h).

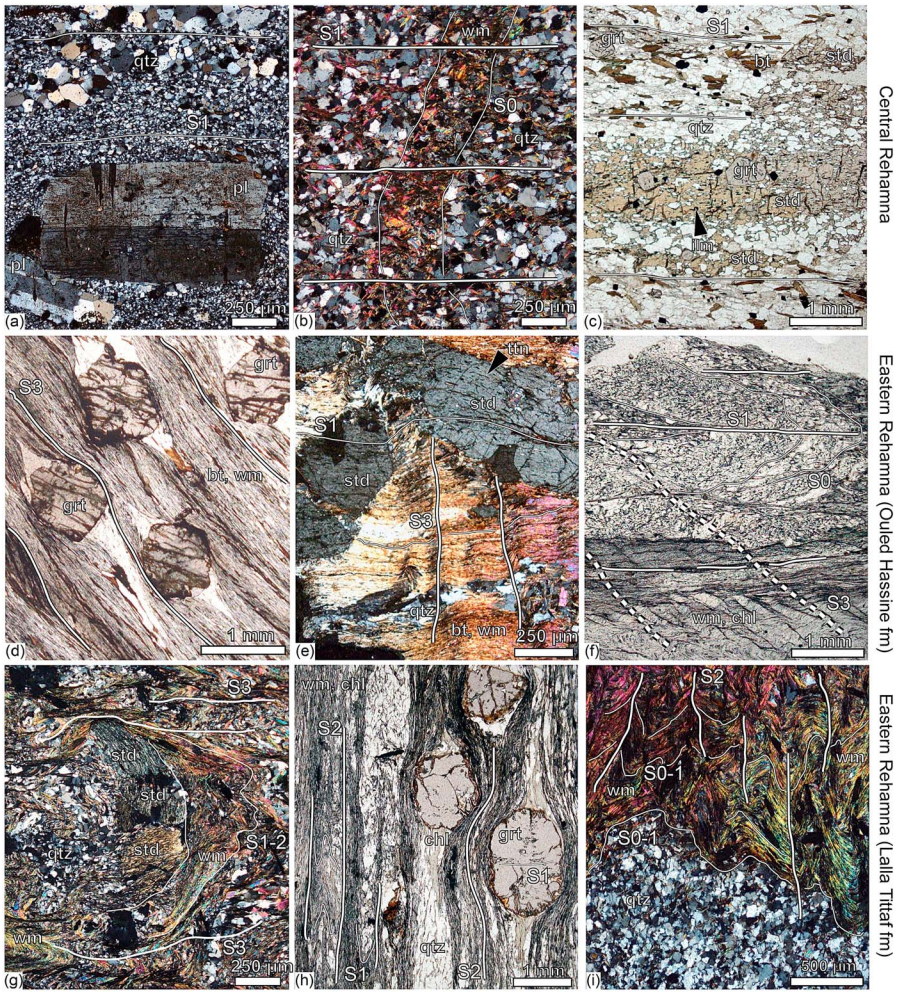

Figure 8. Photomicrographs illustrating the relationships between metamorphic minerals and microstructures in the lower metamorphic unit. (a) Development of the S1 metamorphic foliation in the Lower Cambrian metagreywacke from the Sidi Ali dome. (b) S0 layering reworked by recumbent open F1 fold in Devonian metapelite from Kel El Mouned. (c) Staurolite with garnet inclusions parallel to the S1 metamorphic foliation in mica schist from Lower/Middle Cambrian rocks north of the Sidi Ali dome. (d) Intense shearing around garnet porphyroblast in mica schist from the Ouled Zednes fault zone. (e) Staurolite bearing mica schist with S1 foliation weakly affected by F3 asymmetric folds (Ouled Hassine formation). (f) F1 folds slightly reworked by asymmetric F3 folds in a biotite-bearing mica schist from the Devonian Ouled Hassine formation. (g) S3 crenulation cleavage in mica schist from the Lalla Tittaf formation close to the contact with the Ouled Hassine formation in the Ras El Abiod area. A microlithon containing folded staurolites is visible in the center of the picture. (h) Subvertical S2 crenulation cleavage in garnet-bearing mica schist from the eastern part of the Lalla Tittaf formation. (i) Subvertical S2 crenulation cleavage with compositional layering S0-1 preserved in mica schist from the eastern part of the Lalla Tittaf formation. Abbreviations: Biotite (Bt), Chlorite (chl), Garnet (grt), Plagioclase (pl), Quartz (qtz), Staurolite (std), Ilmenite (ilm), White micas (wm).

Late heterogeneous D3 deformation affects the earlier fabrics and associated minerals. Within the Ouled Zednes fault zone, intense D3 shearing leads to the formation of a mylonitic fabric in which biotite and white micas in the matrix are entirely recrystallized and new chlorite grows in pressure shadows around garnet porphyroclasts (Figure 8d). In contrast, far from this major shear zone, the S1 layering is only slightly folded or kinked (Figure 8e).

D3 deformation is also intense at the southwestern boundary between the Lalla Tittaf and Ouled Hassine formations in the Ras El Abiod area. Here late ductile shearing affects staurolite ± garnet-micaschist leading to the formation of fine-grained mica-rich layers (Figure 8g). This metamorphic recrystallization is penecontemporaneous with the syntectonic intrusion of the Ras El Abiod leucogranite, which shows geometrically coherent solid state mylonitic deformation at its contact with the host rocks [*Diot*, 1989],

whereas static overgrowth of andalusite, tourmaline, and biotite took place in the aureole of contact metamorphism in the pelites of the surrounding area [*Hœpffner et al*., 1982; *Lagarde*, 1989; *Diot*, 1989; *Diot and Bouchez*, 1991; *Lagarde et al*., 1990].

Intrusion of the Sebt-Brikiine granite at the end of the D3 event was accompanied by weak magmatic to brittle deformation whereas the posttectonic growth of cordierite and andalusite is widespread in the surrounding metamorphic aureole [*Lagarde*, 1989; *Diot*, 1989; *Diot and Bouchez*, 1991; *Lagarde et al*., 1990].

Since the work of *Hœpffner et al*. [1975a], numerous authors ascribe the local presence of kyanite to the climax of the Barrovian metamorphism. However, in the Rehamna, kyanite crystals are always associated with late quartz veins. As it has been proposed by *El Mahi et al*. [2000b], we suggest that the formation of this mineral is due to a late hydrothermal event.

5. $^{40}Ar/^{39}Ar$ Geochronology

Rocks from the Rehamna Massif have been sampled for laser step-heating $^{40}Ar/^{39}Ar$ geochronology at the University of Nice Sophia Antipolis (Geoazur laboratory) in order to constrain the history of cooling and exhumation of the massif, as well as the timing of intrusion of the granitoids. The location of the samples is shown in Figure 2, and coordinates are given in the supporting information. Step-release spectra are shown in Figure 9, and details of the analytical procedure and results are given in Tables S1–S12 in the supporting information.

5.1. Upper Carboniferous Metamorphic Cooling Ages

Three samples (Figures 9a–9c) from the lower metamorphic unit in the Central (R061A) and Eastern (R147 and R149A) Rehamna yielded Upper Carboniferous metamorphic ages.

Sample R061A (Figure 9a) was collected from the Lower/Middle Cambrian pelites of the Central Rehamna to the north of Sidi Ali village. The rock has a subhorizontal S1 foliation bearing a NE-SW trending L1 mineral lineation. The metamorphic assemblage contains staurolite and garnet porphyroblasts up to 1 cm in diameter, in equilibrium with a fine-grained matrix of white mica + biotite + ilmenite + equant quartz underlying the foliation. Grains of ilmenite and mica that form inclusions in large garnet and staurolite porphyroblasts are parallel to the foliation. Late S3 crenulation is visible in the matrix and may be associated with chloritization of biotite porphyroblasts. An $^{40}Ar/^{39}Ar$ dating of a biotite yielded two first steps below 290 Ma, followed by a 4 step flat spectrum and a plateau age at 309.4 ± 7.2 Ma (80% of the total ^{39}Ar released). The slightly perturbed spectrum at the first steps at low temperature could evidence of argon loss due to a younger thermal event between 150 and 210 Ma.

Sample R147 (Figure 9b) is a strongly sheared metapelite from the Lalla Tittaf formation in the Eastern Rehamna. In the sampled outcrop the S1 foliation and L1 lineation dip moderately to the NE and are deformed by late F2 kink bands. The foliation in this sample contains fine-grained quartz + feldspar + white mica ± biotite and chlorite. An $^{40}Ar/^{39}Ar$ dating of white mica from this sample gave a relatively flat spectrum after the first three steps and a plateau age at 301.1 ± 6.3 Ma (Steps 4–12, 90% of the total ^{39}Ar released). The slightly perturbed spectrum at the first steps at low temperature could be evidence for an excess of argon, so this age should be considered as a maximum age.

Sample R149A (Figure 9c) is an amphibolite from the Lalla Tittaf formation in the Eastern Rehamna. Here the rock is affected by subvertical, E-W trending S2 cleavage bearing a mineral lineation plunging moderately to the west. Microlithons and S2 cleavage in the studied sample consist of medium grained hornblende ± plagioclase. A hornblende yields a heterogeneous spectrum with a relatively flat section between steps 5 and 7 at 309.0 ± 8.4 Ma (67% of the total ^{39}Ar released). However, the saddle-shaped age spectrum might be due to an excess of argon.

5.2. Permian Metamorphic Cooling Ages

Four samples (Figures 9d–9g) from the lower metamorphic unit in the Central (11-01B) and Eastern (12-02C, R136C, and R079D) Rehamna yielded Permian metamorphic ages.

Sample 11-01B (Figure 9d) is a metarhyolite collected from the Neoproterozoic basement of the Central Rehamna cropping out at Sidi Ali village. Here a strong subhorizontal S1 foliation bearing a NE-SW trending

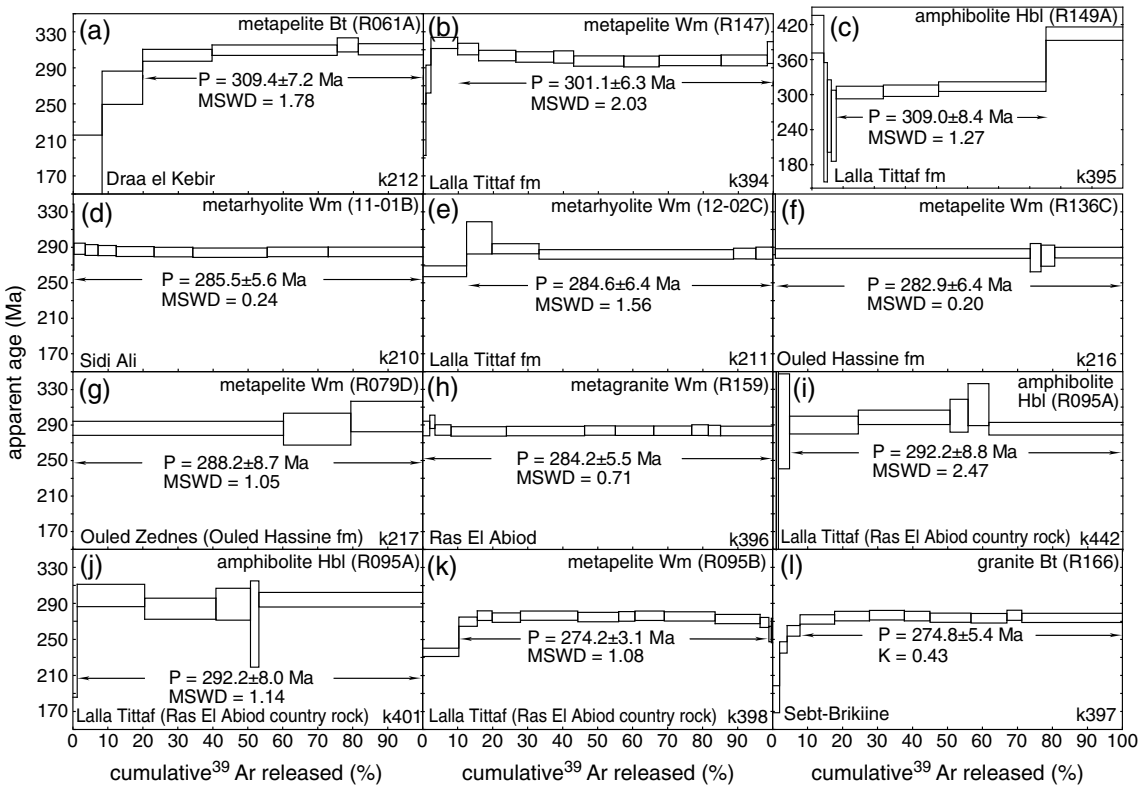

Figure 9. An $^{40}Ar/^{39}Ar$ age spectra as a function of released ^{39}Ar on white mica (Wm), Biotite (Bt), and hornblende (Hbl) single grains of samples from the infrastructure. Rock type and analyzed mineral are given together with the sample number (in brackets) and the analytical reference of the laboratory (bottom right-hand side; see Tables S1–S12 for raw data). The error boxes for each step and for the flat spectrum part ages are at the 2σ level. Ages were calculated using the ArArCalc program of *Koppers* [2002].

stretching lineation is present. A fine-grained matrix is composed of dynamically recrystallized quartz and feldspars alternates with white mica lithons. A white mica from this sample gave a flat spectrum with a plateau age at 285.5 ± 5.6 Ma (2–9 steps, 100% of the total ^{39}Ar released).

Sample 12-02C (Figure 9e) is a metarhyolite from a 300 m wide felsic body within the Lalla Tittaf formation in the Eastern Rehamna. Here moderately SE dipping S3 foliation is characterized by well-developed layering consisting of fine grained dynamically recrystallized quartzo-feldspathic matrix alternating with white mica layers. After a first step lower than 270 Ma, white mica gave a relatively flat age spectrum with a plateau age at 284.6 ± 6.4 Ma (2–6 steps, 87% of the total ^{39}Ar released).

Sample R136C (Figure 9f) is a pelite from the Ouled Hassine formation in the Eastern Rehamna. Here the S1 foliation dips moderately to the ESE, bearing a weak subhorizontal mineral lineation. The metamorphic assemblage consists of staurolite, garnet, biotite, white mica, quartz, and late chlorite. The microstructure of the rock is formed by fine-grained mica and quartz layers with porphyroblasts of staurolite and garnet (up to 2 mm) containing ilmenite inclusions. Some scattered white mica porphyroblasts, up to 100 μm in size, are present. The main foliation is deformed by late F3 kink bands. The age spectrum of this sample shows a first step with an old apparent age up to 290 Ma, followed by a flat spectrum with a plateau age at 282.9 ± 6.4 Ma (2–5 steps, up to 99% of the total ^{39}Ar released).

Sample R079D (Figure 9g) was collected in the Ouled Zednes Fault Zone, in the Ouled Hassine formation. The S1 metamorphic foliation of this pelite is affected by overturned F3 recumbent asymmetrical folds, with S3 cleavage dipping moderately to the east, and fold axes plunging gently to the south. The S3 cleavage is formed by an alternation of white micas, biotite and chlorite layers with recrystallized quartz ribbons. Staurolite porphyroclasts contain parallel to helicitic inclusion trails of ilmenite. The $^{40}Ar/^{39}Ar$ apparent age spectrum from the white mica is flat with a mean age at 288.2 ± 8.7 Ma (3 steps, 100% of the total ^{39}Ar released).

5.3. Cooling Ages of Granitoids and Surrounding Contact Aureoles

One sample (R159) from the Ras El Abiod leucogranite and two samples (R095A and R095B) from the surrounding metamorphic aureole were collected in order to constrain the cooling age of the intrusion. One sample (R166) was collected from the Sebt-Brikiine granite.

Sample R159 (Figure 9h) was collected at the southeastern contact of the Ras El Abiod leucogranite. The granite displays strong foliation dipping moderately to the SSW bearing a lineation dipping gently south. The sample is a protomylonite, with a medium grained matrix consisting of quartz and feldspar with bands of white mica and biotite. Magmatic feldspar phenocrysts show mechanical twinning and are myrmekitic. Magmatic quartz crystals have been completely recrystallized by a process of grain boundary migration. White mica from this sample yields a flat spectrum with a plateau age at 284.2 ± 5.5 Ma (11 steps, 100% of the total ^{39}Ar released).

Samples R095A and R095B (Figures 9i–9k) were collected 200 m away from the previous sample R159 in the country rocks of the Ras El Abiod leucogranite. Here the main S3 foliation is shallowly dipping to the NE and bears strong E-W lineation. Sample R095A is a medium grained amphibolite with a metamorphic assemblage consisting of hornblende, plagioclase, epidote, calcite, and sphene. Sample R095B is a pelite consisting of garnet, white mica, biotite, quartz, and ilmenite. Chlorite has grown in pressure shadows around garnet. Micas are present in the form of grains up to 500 μm in diameter and form layers alternating with quartz lithons. Ilmenite is contained as helicitic inclusions in garnet porphyroclasts. Two analyses of amphiboles from sample R095A show a relatively flat spectrum with a mean age at 292.2 ± 8.8 Ma (steps 4–8, 95% of the total ^{39}Ar released, analysis k442) and 292.2 ± 8.0 Ma (steps 2–6, 98% of the total ^{39}Ar released, analysis k401). After a first lower step, a white mica from the sample R095B yielded a relatively flat spectrum with a plateau age at 274.2 ± 3.1 Ma (steps 2–11, 88% of the total ^{39}Ar released).

Sample R166 (not shown in Figure 2) has been collected from the NE part of the Sebt-Brikiine granite. It is a coarse-grained biotitic granite with phenocrysts of perthitic K-feldspar and a magmatic matrix consisting of plagioclase and quartz with laths of biotite up to 800 μmin length. No magmatic or tectonic fabric is present. After a few steps, the ^{40}Ar/^{39}Ar apparent age spectrum from biotite in this sample remains flat and gives a plateau age at 274.8 ± 5.4 Ma (steps 4–11, 92% of the total ^{39}Ar released). The slightly perturbed spectrum in the first steps at low temperature could be evidence of argon loss due to a younger thermal event (between 170 and 200 Ma).

6. Discussion

The combination of new structural observations and ^{40}Ar/^{39}Ar age determinations presented in this paper has fundamental implications for the interpretation of the tectonic evolution of the Rehamna Massif. Using this information, the events that affected the Rehamna Massif in Morocco can be integrated with the tectonic history of the whole Alleghanian-Variscan orogeny.

6.1. Interpretation of Orogenic Fabrics

Since the work of *Hœpffner et al*. [1975a, 1975b], *Piqué et al*. [1980], and *Michard* [1982], the general architecture of the Rehamna Massif and its tectonic interpretation has been explained in terms of continuous westward accretion of Devono-Carboniferous basins against the Coastal Block. This simple scenario is called into question by the results presented above that suggest a major south-vergent thrusting event was followed by the growth of a crustal dome. The whole crustal edifice was subsequently affected by almost orthogonal ESE-WNW shortening.

6.1.1. D1 Nappe Stacking and Deep Crustal Flow

The strong SSW-SW trending mineral and stretching lineation widely described in the Central Rehamna has been used as a major argument in favor of dextral transpression during displacement of the Coastal Block relative to the Central Zone [e.g., *Lagarde and Michard*, 1986; *Aghzer and Arenas*, 1995; *Baudin et al*., 2003; *Michard et al*., 2010b]. However, alternative interpretations have also been proposed. *Diot* [1989] interpreted these structures as a result of top to the SSW-SW nappe stacking, while *Corsini et al*. [1988a] suggested that tectonic inversion of a Lower Carboniferous basin-related normal fault had taken place. A comparable

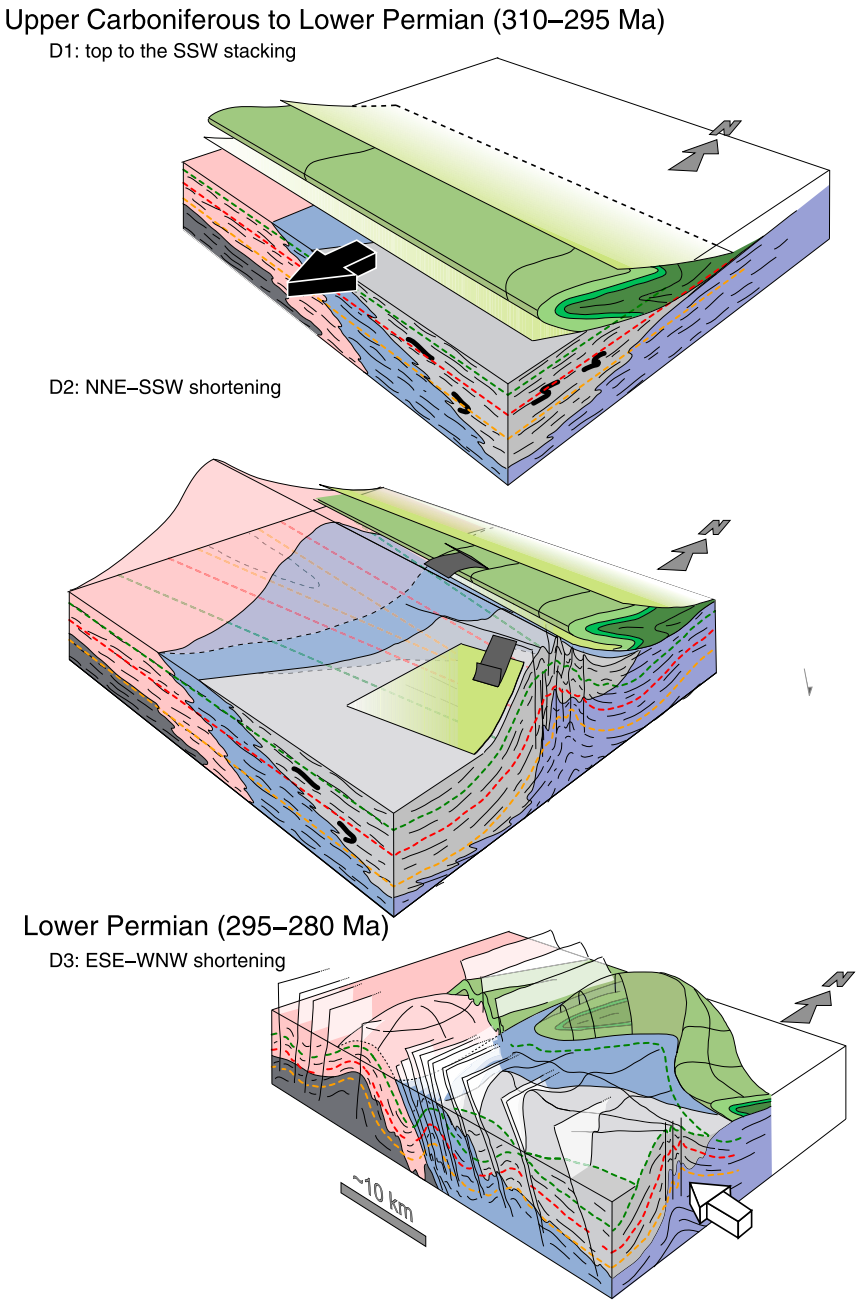

Figure 10. Three-dimensional idealized model for the evolution of the Rehamna Massif (see text for discussion). Colors same as 2.

early stage of southward compression has also been suggested in the Northern Sekhira-es-Slimane Devonian conglomerates close to the Coastal Block [*Piqué*, 1973].

A prograde Barrovian metamorphism is associated with the development of the S1 fabric within the whole lower metamorphic unit [*Aghzer and Arenas*, 1995; *El Mahi et al*., 2000a]. This implies that the S1 foliation is developed in the Devonian and Carboniferous sediments and underlying Neoproterozoic-Lower Paleozoic rocks during burial (Figure 10). The D1 deformation is spatially restricted to the former Devono-Carboniferous basins suggesting structural and probably also thermal inheritance influencing the mode of crustal thickening [*Thompson et al*., 2001]. Here it is argued that the horizontal fabric and prograde metamorphic gradients in the lower metamorphic unit result from the SSW-SW thrusting and imbrication of the Lower Paleozoic sedimentary pile over Devonian and Carboniferous basinal sequences (i.e., southward thrusting of

the Koudiat el Adam-Jbel Kharrou anticline and the Ordovician rocks of the Skhour area) (Figure 10). The consequence of this thrusting is thickening of the crust accompanied by horizontal flow of thermally weakened rocks in an intracontinental rift as proposed, e.g., by *Schulmann et al*. [2002] and *Košuličová and Štípská* [2007] for other parts of the Variscan belt. Consequently, prograde horizontal foliation and metamorphic isograds subparallel to the S1 foliation in the deep crust reflect the horizontal flow accommodating upper crustal thickening. The inheritance of basinal architecture is indicated by the relationship between lithological boundaries and metamorphic isograds [e.g., *Michard et al*., 2010b] shown in Figure 10. In addition, the fact that metamorphic isograds are orthogonal to the D3 Ouled Zedness Fault Zone and tend to be parallel to the D1 thrust in the upper metamorphic Jebel Kharrou and Koudiat al Adam unit [*Michard et al*., 2010b] shows that the pattern of metamorphism is governed by the early ~ E-W trending structures.

The contrast between the style of deformation in the upper and lower metamorphic unit, that is the imbrication, thrusting, and folding at the upper level versus horizontal ductile flow at depth is characteristic of the orogenic superstructure and infrastructure found in metamorphic domes of similar age in the Pyrenees [*van den Eeckhout and Zwart*, 1988].

6.1.2. D2 Synconvergent Doming and Associated Detachments

The continuous SSW-NNE directed compression results in a shortening of the infrastructure that evolves into doming. The synconvergent ~ E-W trending anticline marks the exhumation of the orogenic infrastructure and associated isograds with the deepest metamorphic rocks located in the core of the crustal dome (Figure 10). In its eastern part, this continuous ~ N-S shortening leads to the formation of an upright anticline with a large amplitude and subvertical S2 cleavage, whereas in its western part, the anticline is of smaller amplitude and more open. It is suggested that this difference in amplitude is because the shortening is greater in the weaker Devonian-Carboniferous deep basinal sequences in the east and lesser in the west where a stronger basement is present. Indeed, in the western part of Eastern Rehamna and in the Central Rehamna, the S2 fabric does not develop and the dome structure is defined only by tilting of the S1 fabrics.

In our model, the detachment of the superstructure, i.e., northward sliding of the Koudiat el Adam-Jbel Kharrou anticline is contemporaneous with the synconvergent doming of the infrastructure and not a consequence of an extensional event as proposed by previous authors [*Baudin et al*., 2003; *Razin et al*., 2003]. A similar detachment ought to be present on the southern flank of the developing deep crustal dome.

6.1.3. D3 WNW-ENE Shortening

The D3 event marks a major change in the tectonic regime from SSW-SW directed nappe stacking (D1) and subsequent doming (D2) to a strong D3 WNW-ENE compression. In the infrastructure of the Eastern Rehamna, this is expressed by the formation of large synclines and anticlines [*Baudin et al*., 2003; *Razin et al*., 2003] with an increase in the intensity of deformation toward the west, culminating in thrusting of this unit over the Central Rehamna along the Ouled Zednes fault [*Hœpffner et al*., 1975a, 1975b; *Lagarde and Michard*, 1986]. This thrusting is probably due to the buttressing effect of the rigid Neoproterozoic basement located below the Central Rehamna. In the whole infrastructure, the D3 event is responsible for the folding of D1 isograds, mainly in the west. In contrast, the metamorphic aureole of the Ras El Abiod granite is only elongated parallel to the D3 structural trend (Figure 2).

To the North, the orogenic superstructure formed by the Koudiat el Adam-Jbel Kharrou anticline is moderately refolded and thrust over the Central Rehamna (Sekhira-es-Slimane and Skhour area). Here the D3 folding and intensity of imbrication dramatically increases, suggesting that the rigid Coastal Block behaves as a buttress along the Median fault (Figure 6). In contrast, farther south the interference between F2 and F3 anticlines is responsible for the domal structure in the Central Rehamna and ultimately the exhumation of the Neoproterozoic basement (Sidi Ali).

Previously, the strong lineation developed between the Ouled Zednes and Median faults (Figure 5) has been interpreted as a result of intense strike-slip shearing within the Central Rehamna [*Hœpffner et al*., 1975a, 1975b; *Lagarde and Michard*, 1986] forming part of the main dextral Western Meseta Shear Zone [*Michard et al*., 1978; *Piqué et al*., 1980]. In contrast, it is proposed here that these linear structures result from ~ ESE-WNW shortening of an originally subhorizontal fabric bearing a ~ SWW-SW lineation inherited from the D1 event [see also *Diot*, 1989]. This superposition of strain resulted in the development of subhorizontal prolate ellipsoidal geometries as illustrated by the spectacular rodding of the Devonian conglomerates at Kef el Mouneb (Figure 5d).

6.1.4. Is the WMSZ a Major Tectonic Boundary?

Based on the interpretation of D3 structures given above, it is argued that the importance of dextral shearing in the Central Rehamna and the role of the WMSZ, in general, has been overestimated. The formation of the WMSZ is best explained as the result of WNW thrusting of the Central Zone of the Western Meseta over the Coastal Block [see also *Baudin et al*., 2003] rather than by dextral shearing between two independent terranes. The localized thrusting is due to the buttress effect of the underlying Neoproterozoic basement. In addition, the Eastern Rehamna is thrust over the Central Rehamna along the Ouled Zednes Fault [*Baudin et al*., 2003]. As a consequence, the D3 deformation is localized within the Central and Eastern Meseta along the western border of the Devono-Carboniferous basin. The D3 deformation zone simply reflects the structural inheritance of originally NNE-SSW trending sedimentary basins developed on the Lower Paleozoic cover of the Neoproterozoic basement and is not a major transpressive boundary between different terranes.

This explains similarities between the Lower Paleozoic successions of the Coastal Block and the Meseta which have long been recognized and suggests that there is not a major break between the two regions [*Destombes et al*., 1985; *Hœpffner et al*., 2005; *Michard et al*., 2008]. The siliciclastic sedimentary sequences of both regions appear to have developed in an epicontinental platform environment on the main Gondwana landmass, showing evidence of the same Lower Paleozoic marker events including Lower-Middle Cambrian rifts [*Bernardin et al*., 1988; *Piqué*, 2003; *Pouclet et al*., 2008], the Lower Ordovician hiatus [*Ghienne et al*., 2007], and the end-Ordovician glaciation [*Le Heron et al*., 2007]. Differences between the stratigraphies of the Coastal Block (Western Rehamna) and those of the Central Rehamna (Western Meseta) are less striking than those occurring within the Meseta block itself. Based on its evolution during the Lower Paleozoic, the whole area appears to have formed a single, but composite, domain [*Michard et al*., 2008].

6.2. Timing of Tectonic and Magmatic Events

The $^{40}Ar/^{39}Ar$ geochronological study has yielded three groups of ages that constrain (1) the D1 SSW-SW directed nappe stacking and subsequent D2 doming, (2) the D3 WNW-ESE compression accompanied by syntectonic intrusions, and (3) the late magmatic posttectonic event.

6.2.1. Significance of Upper Carboniferous Ages

The ~309 ± 7 Ma (sample R061, Figure 9a) and ~301 ± 6 Ma (sample R147, Figure 9b) $^{40}Ar/^{39}Ar$ ages were obtained from metamorphic white micas from the garnet-biotite and staurolite metamorphic zones. The metamorphic temperatures for the two samples can be estimated as 450 and 550°C, respectively. They are therefore far above the blocking temperature of ~360°C for argon diffusion in muscovite [*Dodson*, 1973]. Therefore, these two ages probably indicate the time of cooling of the metamorphic rocks when they were exhumed during the formation of the D2 anticline. The amphibolite from the Lalla Tittaf formation (sample R149A, Figure 9c) that yielded an $^{40}Ar/^{39}Ar$ plateau age of ~309 ± 8 Ma was collected from the biotite-garnet zone, and the blocking temperature of hornblende ~ 500°C is therefore close to the peak metamorphic temperature. This implies that this age may be close to the D1 metamorphic age but it is from a region with the strongest D2 structural overprint. Therefore, we suggest that Upper Carboniferous ages of this study mainly reflect the formation of the Rehamna dome during D2. The preservation of D1 and D2 cooling ages is also supported by the location of samples R147 and R149 which both lie in the low-grade part of Eastern Rehamna where the effect of late D3 deformation is negligible or absent. The D2 doming and exhumation of the deep infrastructure can have taken place soon after the south-vergent D1 folding and thrusting and the formation of the infrastructure and superstructure pattern.

6.2.2. Significance of Lower Permian Ages

The $^{40}Ar/^{39}Ar$ ages ~285 ± 5 Ma (sample 11-01B, Figure 9d) and ~283 ± 6 Ma (sample R136C, Figure 9f) obtained from the Sidi Ali dome and the Ouled Hassine formation are interpreted to be the result of resetting of the argon system during the D3 event. This hypothesis is confirmed by an $^{40}Ar/^{39}Ar$ muscovite age of 288 ± 9 Ma for sample R079D from the strongly retrogressed schists within the Ouled Zednes fault zone (Figure 9g), and by the $^{40}Ar/^{39}Ar$ muscovite age of ~285 ± 6 Ma from a sample located at the southwestern boundary between Ouled Hassine and Lalla Tittaf formation also strongly affected by D3 deformation and muscovite neocrystallization (sample 12-02C, Figure 9e). These results indicate that the D3 event is responsible for resetting the argon system in muscovite during a major but heterogeneous reworking of the eastern part of Eastern and Central Rehamna.

The timing of D3 is confirmed by the $^{40}Ar/^{39}Ar$ muscovite age of ~284 ± 5 Ma from the deformed Ras El Abiod granite (sample R159, Figure 9h) and the $^{40}Ar/^{39}Ar$ muscovite age of ~292.23 ± 8 Ma (sample R095A, Figures 9i and 9j) from rocks affected by D3 retrogression in the contact aureole of the granite massif. These two ages are interpreted to be the time of crystallization of the syntectonically emplaced granite and its thermal metamorphism of the host rock during D3 deformation. The zircon U-Pb crystallization age of 285 ± 6 Ma for the Ras El Abiod intrusion [*Baudin et al*., 2003] and reopening of the isotopic system in zircons from the metagabbros of the Lalla Tittaf formation at 284 ± 6 Ma demonstrates that granite cooling and D3 deformation occurred almost simultaneously. Indeed, a small granite stock emplaced at upper crustal levels will cool in a time of the order of a hundred thousand years as shown for instance by *Kratinová et al*. [2007]. Consequently, we suggest that the D3 event is Lower Permian (Autunian) with a climax at 285 Ma even though deformation may have started earlier at the Permo-Carboniferous boundary (~295–300 Ma).

6.2.3. Age of the Post-D3 Granitoid

The muscovite 275.8 ± 5 Ma $^{40}Ar/^{39}Ar$ plateau age obtained for the Sebt-Brikiine granitoid corresponds to the emplacement of this late-tectonic batholith (sample R166, Figure 9l). It is slightly older than the Rb-Sr age obtained by *Mrini et al*. [1992] (268 ± 6 Ma) but similar to the 278 ± 2 Ma age of the associated dykes obtained using the same method (Tisserant [1977] in *Hœpffner et al*. [1982]). The emplacement of this pluton postdates F3 folding of the Lower Paleozoic sequences in the Coastal Block suggesting that the age ~276 Ma may be considered as an upper limit of D3 deformation.

6.3. The Rehamna in the Context of the Moroccan Variscides

6.3.1. Lower Carboniferous Opening of Intracontinental Basins (345–315 Ma)

Volcano-clastic basins in the Eastern Meseta postdate the Eo-Variscan (i.e., Upper Devonian-Tournaisian) deformation and show presence of calc-alkaline magmatism dated at 345 and 320 Ma (U-Pb on zircon, *Oukemeni et al*. [1995]; $^{87}Sr/^{86}Sr$ versus Rb-Sr isochrones, *Ajaji et al*. [1998]). Simultaneously, intracontinental basins with interstratified bimodal magmatism formed throughout the whole Western Meseta [*Hœpffner et al*., 2006b, and references therein]. In these basins, the Visean to early Serpukhovian sedimentation [e.g., *Playford et al*., 2008; *González et al*., 2011] is contemporaneous with a thermal event dated at 330–320 Ma in the Central Massif ([*Huon et al*., 1987]; white mica K-Ar ages on slates). It is also coeval with the magmatic activity and fluid circulations in the Jebilet as shown by the emplacement of cordierite-bearing granodiorites at ~327 Ma (Rb-Sr isochrones, *Mrini et al*. [1992]) and a granitic sill emplaced at ~330 Ma (U-Pb zircon, [*Essaifi et al*., 2003]), together with sulphide deposits dated at ~332 Ma by $^{40}Ar/^{39}Ar$ method on hydrothermal sericite [*Marcoux et al*., 2008]. These Carboniferous basins in Western Meseta are interpreted as foreland basins related to north-westward propagation of thrusts and folds [*Ben Abbou et al*., 2001; *Roddaz et al*., 2002], or intraplate extensional basins [*Hœpffner et al*., 2005, 2006b, and references therein]. Recently, *Tahiri et al*. [2010] suggested that these basins can be opened during the southward docking of the Sehoul block against the Western Meseta.

6.3.2. NE-SW to NNE-SSW Shortening During Upper Carboniferous to Lower Permian (310–295 Ma)

In the Eastern Meseta, Westphalian deformation resulted in formation of mostly ENE-WNW striking folds and foliation [*Huon et al*., 1987] associated with anchizonal metamorphism [*Hœpffner*, 1987; *Erraji*, 1997; *Houari and Hœpffner*, 2003; *Hœpffner et al*., 2005]. Few syntectonic granitoids emplaced shortly before and during this tectonic event at circa 320–300 Ma [*Diot and Bouchez*, 1991; *El Hadi et al*., 2006, and references therein].

Previous studies proposed that the Westphalian deformation in the Western Meseta relates only to a NW-SE to WNW-ESE compression [*Michard et al*., 2010b, and references therein]. However, we suggest that the earliest deformation fabrics in the Rehamna (D1 and D2) are compatible with a NNE-SSW convergence from the Westphalian to the Lower Autunian (i.e., 310–295 Ma). In this revised model, the SSW directed movement postdates sedimentation in the Visean to early Serpukhovian basins and is thus not connected to their formation as proposed by *Essaifi et al*. [2014] in the Jebilet. In the Central Massif, the folds and foliation trends form a V-shape structure which is parallel to the Sehoul block boundary (Figure 1). This structural pattern was attributed to an inherited rhomboidal shape of Carboniferous basins which have been inverted during NW-SE to WNW-ESE compression along the WMSZ [e.g., *Piqué et al*., 1980]. In contrast, we propose that WNW-ESE fabric trend in front of the Sehoul block (Figure 1) results from a buttress effect related to its SSW movement. Subsequent propagation of deformation in front to SSW moving indentor may be responsible for the south-vergent thrusting observed in the Central Massif [*Hœpffner*, 1987], formation of (D1 and D2) early WSW-ENE trending fabrics in the Rehamna and in

Jebilet [*Boummane and Olivier*, 2007], the latter being also extruded in a general NE-SW to NNE-SSW synconvergent extensional context [*Essaifi et al*., 2014]. Altogether, these observations indicate that the southward compression is a major regional feature and affects a large portion of Moroccan Meseta as well as its southern border in the High Atlas [*Pouclet et al*., 2008].

6.3.3. NW-SE to WNW-ESE Shortening During Lower Permian (295–280 Ma)

In the Eastern Meseta, the emplacement of Lower Permian calco-alcaline granitoids dated at ~284–287 Ma (Rb-Sr ages, [*Tisserant* 1977; *Mrini et al*., 1992]) is considered to be postcollisional [*El Hadi et al*., 2003]. However, in the Central Massif, the granitoids dated at circa 291 and 296 Ma (U-Pb zircon ages, [*Chèvremont et al*., 2001; *Baudin et al*., 2001]) are emplaced at the end of the WNW-ESE compressive event [*Diot and Bouchez*, 1991; *Tahiri et al*., 2007]. These results corroborate the syntectonic emplacement of the Ras El Abiod granite at circa 295 and 285 Ma in the Rehamna Massif, leucogranite sheet dated at circa 295 Ma in the Jebilet (Rb-Sr isochron, [*Mrini et al*., 1992]) and intrusion of the Tichka granite in High Atlas dated at circa 291 and 283 Ma using Rb-Sr and Sm-Nd isochrons, respectively [*Gasquet et al*., 1992]. Based on all these data, we suggest that D3 shortening event in the Rehamna corresponds to a major Permian NW-SE to WNW-ESE shortening affecting the whole Western Meseta.

6.3.4. Late to Postorogenic Magmatism (280−260 Ma)

In the Rehamna Massif, the intrusion of the Sebt-Brikiine granite and associated dikes at circa 276 Ma postdates ductile deformation. Similar posttectonic intrusions, mostly subalcaline, are widespread in Western Meseta, in particular in the Central Massif where they have been dated using the Rb-Sr method (whole rock) by *Mrini et al*. [1992]. All of these intrusions represent late to postorogenic magmatic events.

6.4. The Rehamna and the Moroccan Variscides in the Context of the Alleghanian-Variscan Orogeny

A number of large-scale correlations between the Variscan Orogeny in Europe and northwestern Africa and the Alleghanian (Appalachian) belt in North America have been proposed [*Arthaud and Matte*, 1977; *Piqué*, 1981; *Matte*, 2001; *Houari and Hœpffner*, 2003; *Hœpffner et al*., 2005, 2006a, 2006b; *Simancas et al*., 2005; *Engelder and Whitaker*, 2006; *Michard et al*., 2008; *Simancas et al*., 2009; *Hatcher*, 2010]. Except for a few structural studies of the Appalachian orogeny in the eastern United States [e.g., *Hatcher*, 2010; *Engelder and Whitaker*, 2006] and in southern Europe [*Edel et al*., 2013; *Weil et al*., 2013], the early stages of deformation are not taken into account and most of the cited studies focus on late structures. To fill this gap, observations from the Rehamna Massif have been used as the basis for a two-stage history of geodynamic evolution taking into account comparable data from southern Europe and North America (from the Upper Carboniferous to the Lower Permian, Figure 11).

6.4.1. Upper Carboniferous to Lower Permian

The birth of the Alleghanian orogeny (Appalachian, North America) starts with major dextral strike-slip movements and local thrusting during the Upper Mississippian (<325Ma [*Hatcher*, 2010]). This is concordant with the orientation of the maximum horizontal stress within the Southern and Central Appalachians based on the strike of joints within coal-bearing sediments formed between 305 and 290 Ma (Appalachian-wide stress field of *Engelder and Whitaker* [2006]). This major dextral shearing took place between margins of Laurentia and Gondwana [*Coward*, 1993] and is associated in Appalachian with syntectonic intrusions and metamorphism [*Hermes and Murray*, 1988; *Hatcher et al*., 2007], in particular in New England where partial melting affects the orogenic middle crust at circa 300–290 Ma [*Walsh et al*., 2007].

At the same time, in Europe, the French Massif Central was affected by the synconvergent E-W oriented collapse of the thickened Variscan crust associated with intrusion of numerous syntectonic plutons [*Faure*, 1995; *Faure et al*., 2009, and references therein]. However, orogen-parallel extension in the French Massif Central operated simultaneously with thrusting along the northern margin of the central Armorican domain [*Lacquement et al*., 2005; *Ballèvre et al*., 2009] while E-W synconvergent gneiss domes were growing in the south in the Montagne Noire and Pyrenean regions [*Denèle et al*., 2009; *Charles et al*., 2009]. Further south, the Iberia Orocline was developing due to N-S shortening at 310–295 Ma [*Gutiérrez-Alonso et al*., 2011, 2012]. The southward propagation of this deformation probably resulted in the thrusting of the Sehoul block over the Meseta domain [*Tahiri et al*., 2010].

The D1 metamorphism, horizontal flow and D2 E-W doming observed in the Rehamna dome at 310–295 Ma can be kinematically and chronologically correlated with the growth of similar domes in the Pyrenees [*Denèle et al*., 2007, 2014] and the Montagne Noire [*Charles et al*., 2009] and also with the formation of the Iberian

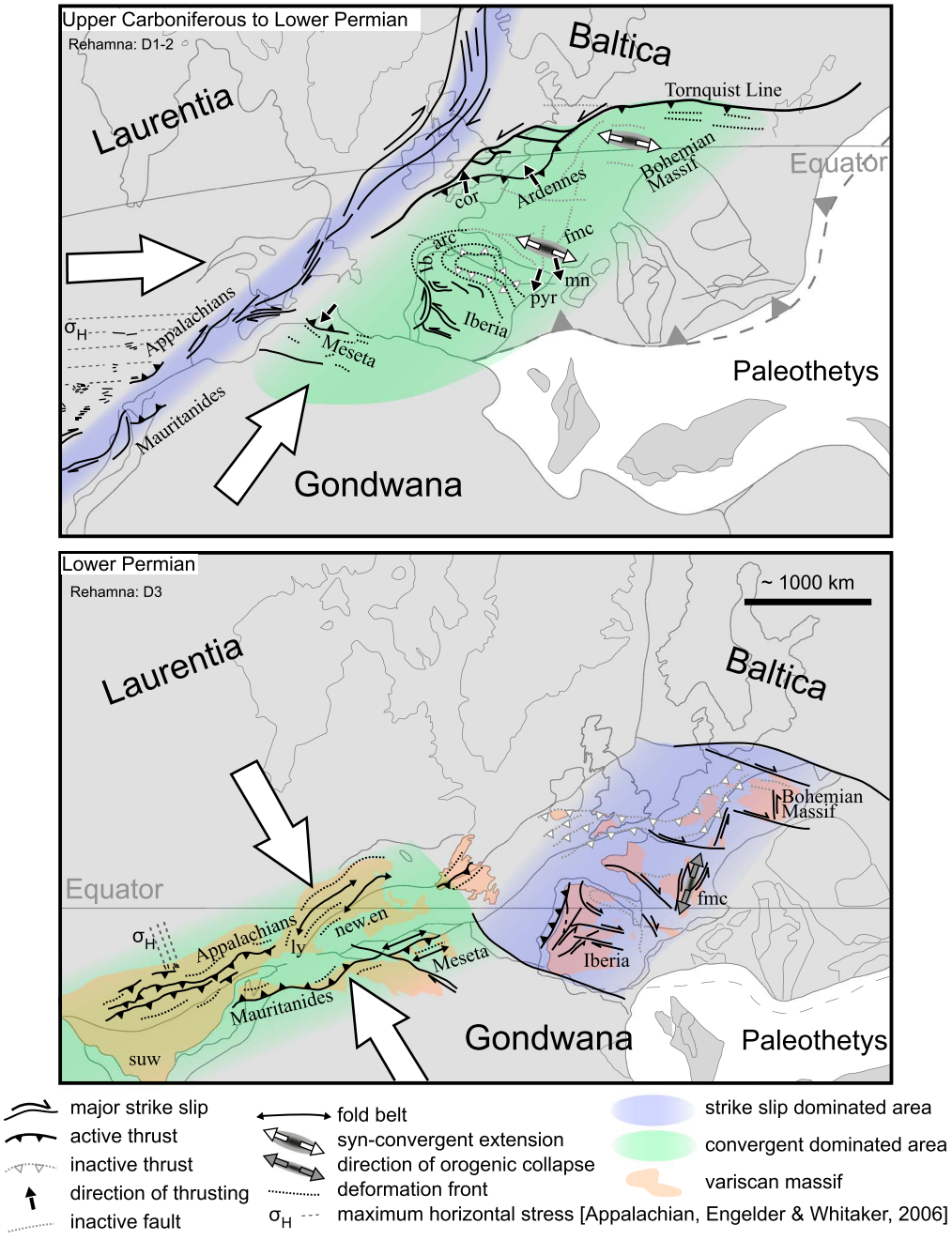

Figure 11. Tectonic evolution of the studied area in the frame of the Alleghanian-Variscan orogeny, see text for discussion and references. Palaeogeographic reconstructions at 310 and 280 Ma after *Cocks and Torsvik* [2006], tectonic structures in North America after *Hatcher* [2010]. Abbreviations: Pyrenees (Pyr), Iberian arc (Ib. arc), Montagne Noire (mn), French Massif Central (fmc), Cornwall (cor), New England (new.eng), Lyme dome (ly), and Suwannee terrane (suw).

orocline [*Gutiérrez-Alonso et al.*, 2011, 2012; *Weil et al.*, 2013]. The timing and structural style characterized by horizontal flow in the infrastructure, imbrication and folding of the superstructure and subsequent formation of crustal domes are identical in Morocco and the Pyrenees. Thus, southern Europe and North Morocco both underwent deformation in which identical structures developed at the same time suggesting collision of north Gondwana with the previously assembled Variscan belt in the Upper Carboniferous [*Edel et al.*, 2013, 2014]. Frontal convergence of Gondwana and the Variscan collage in the north took place at the same time as the whole system was undergoing dextral shearing parallel to the margin of Laurentia in agreement with the model

of *Hatcher* [2010]. Therefore, at the scale of lithospheric plates, two major domains can be distinguished (1) the zone of dextral translation of Gondwana parallel to the boundary of Laurentia, and (2) a zone of frontal collision between the Variscan collage in Europe and Gondwana (Figure 11).

6.4.2. Lower Permian

Major changes in the tectonic regime occurred during the Lower Permian (Figure 11). For instance, the Alleghanian fold-and-thrust belt in the Appalachians formed as a result of head-on tectonics due to an ESE-WNW contraction [*Hatcher*, 2010]. From 290 Ma, in Southern and Central Appalachian, the younger joint set formed in the coal-bearing sediments indicates a new orientation of the maximum compressional stress which is parallel to the direction of Permian thrusting [*Engelder and Whitaker*, 2006]. During this shortening, syntectonic magmatism and metamorphism are still active throughout Appalachian [*Hatcher et al*., 2007], for instance in New England [*Eusden and Barreiro*, 1988; *West et al*., 1988] where synconvergent extrusion of the Lym dome and coeval granitic intrusions took place at circa 290–280 Ma [*Walsh et al*., 2007]. Contemporaneous intrusions have been also found in the Gondwana-derived Suwannee terrane at circa 295 Ma in Southern Appalachian [*Heatherington et al*., 2010].

This event can be directly compared to that affecting the Moroccan Meseta which was subject to ESE-WNW compression during D3 at 295–280 Ma as indicated by the $^{40}Ar/^{39}Ar$ ages reported above in this paper. In addition, similar $^{40}Ar/^{39}Ar$ ages of 290–270 Ma are reported from mylonitic thrust zones in the southern Mauritanide belt suggesting that this event affected the whole Gondwana-Laurentia margin (Lecorché in *Caby and Kienast* [2009]). However, the deformation regime is quite different in the European Variscan collage in Europe. In Iberia, dextral shearing parallel to the Gondwana boundary and conjugate sinistral shear zones are dominant [*Ribeiro et al*., 2007; *Carreras and Druguet*, 2014]. Indeed, the Lower Permian is characterized by shear zone activity throughout Variscan Europe [*Arthaud and Matte*, 1977; *Brandmayr et al*., 1995] accompanied by the formation of numerous Permian basins [*Burg et al*., 1994] and granitoids [*Wilson et al*., 2004]. According to *Arthaud and Matte* [1977], the European Variscan collage was affected by large-scale dextral shearing related to the westward movement of Gondwana.

The evidence presented and discussed above indicates that the Alleghanian orogeny in the eastern United States and the Permian deformation of north Morocco was caused by a kinematically and temporally identical shortening event. On both sides of the Atlantic, this event is characterized by large-scale upright folding and thrusting suggesting frontal collision in an ESE-WNW direction (relative to present geographical coordinates) between Laurentia and Gondwana. At the same time, the Variscan collage in Europe experienced lithosphere-scale dextral shearing parallel to the northern margin of Gondwana. Consequently, it is the frontal ESE-WNW convergence of Gondwana and Laurentia which is responsible for the formation of the continental-scale dextral transfer zone affecting most of the European crust during the Permian. Therefore, as during the Carboniferous, two major kinematic domains at the scale of lithospheric plates can be distinguished (1) the zone of frontal collision between Laurentia and Gondwana and (2) a zone of dextral shearing between the Variscan collage in Europe and Gondwana. Finally, posttectonic thermal and magmatic activity, bracketed in Rehamna at 275 Ma, is also present in adjacent Meseta massifs [*Mrini et al*., 1992], in Appalachian [*Zartman and Hermes*, 1987; *Goldsmith*, 1988; *Walsh et al*., 2007], and in European Variscan belt [*Schuster and Stüwe*, 2008].

7. Conclusion

The combined structural and geochronological studies of the Rehamna Massif have shed new light on the tectonic evolution of the Moroccan Variscan belt leading to the following conclusions:

1. The Rehamna metamorphic dome was formed in two stages starting with crustal thickening of the Devonian and Carboniferous sedimentary basin associated with thrusting and folding in the upper crustal levels under a regime of south directed stress. The SSW-directed compressional deformation evolved continuously leading to the formation of the ~ E-W trending Rehamna dome during Upper Carboniferous. The Upper Carboniferous ~ N-S shortening is comparable to the kinematically and geochronologically identical event in Europe, suggesting frontal convergence of the Gondwana landmass with the European Variscan collage to the north. At the same time the eastern margin of Laurentia was undergoing dextral strike-slip deformation.
2. Lower Permian compression orthogonal to the preceding deformation resulted in westward thrusting of the whole dome over the adjacent continental block. This event resulted in major shortening and refolding of the Rehamna dome.

3. This Lower Permian event in Morocco is correlated with the E-W Alleghanian folding and thrusting affecting the Laurentian margin while Europe was subject to major dextral wrench deformation.
4. The tectonic switch affecting the Moroccan Variscides reflects major change in plate configuration at the Carboniferous-Permian boundary and provides a clue to the understanding of the final suturing of Pangaea.

Acknowledgments
The institutional funding received by F.C. from the Institut de Physique de Globe de Strasbourg, University of Strasbourg (UMR 7516) and the University of Nice Sophia Antipolis (Geoazur, UMR6526) is gratefully acknowledged. This paper is a contribution to the LK11202 program funded through an award to K.S. by the Ministry of Education of the Czech Republic. Ahmed El Attari from the Université Chouaib Doukkali provided valuable assistance in the field, and Sylvain Gallet is acknowledged for supervising the $^{40}Ar/^{39}Ar$ dating at the University of Nice Sophia Antipolis.

References

Aghzer, A. M., and R. Arenas (1995), Détachements et tectonique extensive dans le massif hercynien des Rehamna (Maroc), *J. Afr. Earth Sci.*, *21*(3), 383–393, doi:10.1016/0899-5362(95)00096-C.

Aghzer, A. M., and R. Arenas (1998), Evolution métamorphique des métapélites du Massif hercynien des Rehamna (Maroc): Implications tectonothermales, *J. Afr. Earth Sci.*, *27*(1), 87–106, doi:10.1016/S0899-5362(98)00048-7.

Ajaji, T., D. Weis, A. Giret, and M. Bouabdellah (1998), Coeval potassic and sodic calc-alkaline series in the post-collisional Hercynian Tanncherfi intrusive complex, northeastern Morocco: Geochemical, isotopic and geochronological evidence, *Lithos*, *45*, 371–293, doi:10.1016/S0024-4937(98)00040-1.

Arthaud, F., and P. Matte (1977), Late Paleozoic strike-slip faulting in southern Europe and northern Africa: Result of a right-lateral shear zone between the Appalachians and the Urals, *Geol. Soc. Am. Bull.*, *88*(9), 1305–1320, doi:10.1130/0016-7606(1977)88<1305:lpsfis>2.0.co;2.

Ballèvre, M., V. Bosse, C. Ducassou, and P. Pitra (2009), Palaeozoic history of the Armorican Massif: Models for the tectonic evolution of the suture zones, in *Mechanics of Variscan Orogeny: A modern View on Orogenic Research*, *C.R. Geosci.*, vol. 341, edited by K. Schulmann et al., pp. 174–201, Elsevier Science, Paris, doi:10.1016/j.crte.2008.11.009.

Baudin, T., P. Chèvremont, P. Razin, D. Thiéblemont, H. Rachdi, R. Benhaourch, and A. Winckel (2001), Carte géologique du Maroc au 1/50000, feuille d'Oulmès, Mémoire explicative, *Notes et Mémoires du Service Géologique du Maroc*, *410*, 1–77.

Baudin, T., P. Chèvremont, P. Razin, N. Youbi, D. Andries, C. Hœpffner, D. Thiéblemont, E. Chihani, and M. Tegyey (2003), Carte géologique du Maroc au 1/50 000, feuille de Skhour des Rehamna, Mémoire explicatif, *Notes et Mémoires du Service Géologique du Maroc*, *435*, 1–114.

Ben Abbou, M., et al. (2001), Contrôle tectonique de la sédimentation dans le système de bassins d'avant-pays de la Meseta marocaine. Controls of deposition by thrust-propagation folds in the Moroccan Meseta foreland basin system, *Comptes Rendus de l'Académie des Sciences, Paris, Série IIA*, *332*(11), 703–709, doi:10.1016/S1251-8050(01)01590-7.

Bernardin, C., J.-J. Cornée, M. Corsini, S. Mayol, J. Muller, and M. Tayebi (1988), Variations d'épaisseur du Cambrien moyen en Meseta marocaine occidentale: Signification géodynamique des données de surface et de subsurface, *Can. J. Earth Sci.*, *25*, 2014–2117, doi:10.1139/e88-194.

Bouabdelli, M., and A. Piqué (1996), Du bassin sur décrochement au bassin d'avant-pays: Dynamique du bassin d'Azrou-Khénifra (Maroc hercynien central), *J. Afr. Earth Sci.*, *23*(2), 213–224, doi:10.1016/S0899-5362(96)00063-2.

Boulin, J., M. Bouabdelli, and M. El Houicha (1988), Evolution paléogéographique et géodynamique de la chaîne Paléozoïque du Moyen-Maroc: Un essai de modélisation, *Comptes Rendus de l'Académie des Sciences, Paris Série II*, *306*(20), 1501–1506.

Boummane M. H. and P. H. Olivier (2007), The Oulad Ouaslam Variscan granitic pluton (Jebilets Massif, Southwestern Moroccan Meseta): A forcibly emplaced laccolithic intrusion characterized by its magnetic and magmatic fabrics, *J. Afr. Earth Sci.*, *47*, 49–61, doi:10.1016/j.jafrearsci.2006.10.004.

Brandmayr, M., R. D. Dallmeyer, R. Handler, and E. Wallbrecher (1995), Conjugate shear zones in the Southern Bohemian Massif (Austria): Implications for Variscan and Alpine tectonothermal activity, *Tectonophysics*, *248*(1–2), 97–116, doi:10.1016/0040-1951(95)00003-6.

Burg, J.-P., J. Van Den Driessche, and J.-P. Brun (1994), Syn to post-thickening extension in the Variscan Belt of Western Europe: Modes and structural consequences, *Géologie de la France*, *3*, 33–51.

Burkhard, M., S. Caritg, U. Helg, C. Robert-Charrue, and A. Soulaimani (2006), Tectonics of the Anti-Atlas of Morocco, *C. R. Geosci.*, *338*(1–2), 11–24, doi:10.1016/j.crte.2005.11.012.

Caby, R., and J. R. Kienast (2009), Neoproterozoic and Hercynian metamorphic events in the Central Mauritanides: Implications for the geodynamic evolution of West Africa, *J. Afr. Earth Sci.*, *53*(3), 122–136, doi:10.1016/j.jafrearsci.2008.09.004.

Carreras, J., and E. Druguet (2014), Framing the tectonic regime of the NE Iberian Variscan segment, in *The Variscan Orogeny: Extent, Timescale and the Formation of the European Crust*, edited by K. Schulmann et al., *Geol. Soc. London Spec. Publ.*, *405*, doi:10.1144/SP405.7.

Charles, N., M. Faure, and Y. Chen (2009), The Montagne Noire migmatitic dome emplacement (French Massif Central): New insights from petrofabric and AMS studies, *Terra Nova*, *19*, 445–453, doi:10.1111/j.1365-3121.2007.00770.x.

Chèvremont, P., Y. Cailleux, T. Baudin, P. Razin, D. Thiéblemont, C. H. Hœpffner, A. Bensahal, and R. Benhaourch (2001), Carte géologique du Maroc au 1/50000, feuille d'Ezzhiliga, Mémoire explicatif, *Notes et Mémoires du Service Géologique*, *413*, 1–93.

Cocks, L. R. M., and T. H. Torsvik (2006), European geography in a global context from the Vendian to the end of the Palaeozoic, in *European Lithosphere Dynamics*, edited by D. G. Gee, *Mem. Geol. Soc. London*, *32*, 83–95, doi:10.1144/GSL.MEM.2006.032.01.05.

Cornée, J.-J. (1982), Étude lithostratigraphique et tectonométamorphique des Rehamna sud-orientales, Plissements et nappes. Contribution à la connaissance de la chaîne hercynienne en Meseta marocaine, Thèse 3^{e} cycle, 175 pp., Travaux des Laboratoires des Sciences de la Terre, Saint Jérôme, Université Aix-Marseille III, Aix-Marseille, France.

Cornée, J.-J., and J. Muller (1981), Évolution tectonique des roches métamorphiques de la partie orientale du massif hercynien des rehamna (Maroc), *Comptes Rendus de l'Académie des Sciences, Paris, Série II*, *293*, 453–455.

Cornée, J.-J., J. Muller, and J. Sougy (1982), Styles et âges de mise en place des nappes hercyniennes dans le Massif des Rehamna orientales (Maroc), *Comptes Rendus de l'Académie des Sciences, Paris, Série II*, *294*, 1107–1110.

Corsini, M. (1988), Relation entre la marge du bassin cambrien et la cinématique hercynienne de la Meseta occidentale du Maroc: Un exemple de l'influence de l'héritage tectono-sédimentaire dans une chaîne intracontinentale, Thèse 3^{e} cycle, 163 pp., Travaux des Laboratoires des Sciences de la Terre, Saint Jérôme, Université Aix-Marseille III, Marseille, France.

Corsini, M., J.-J. Cornée, J. Muller, and A. Vauchez (1988a), Cisaillement ductile synmétamorphe et déplacement tangentiel vers le SW dans les Rehamna (Maroc hercynien), *Comptes Rendus de l'Académie des Sciences, Paris, Série II*, *306*, 1389–1394.

Corsini, M., J. Muller, J.-J. Cornée, and H. Diot (1988b), Découverte de la série basale du Cambrien et de son substratum dans les Rehamna Centraux, haut-fond au Cambrien (Méséta marocaine). Prémices de l'orogenèse hercynienne, *Comptes Rendus de l'Académie des Sciences, Paris, Série II*, *306*, 63–68.

Coward, M. P. (1993), The effect of Late Caledonian and Variscan continental escape tectonics on basement structure, Paleozoic basin kinematics and subsequent Mesozoic basin development in NW Europe, in *Petroleum Geology of Northwest Europe: Proceedings of the 4th Conference*, *Geol. Soc. Petrol. Geol. Conf. Ser.*, vol. 4, edited by J. R. Parker, pp. 1095–1108, Shell UK Exploration and Production London, doi:10.1144/0041095.

Denèle, Y., P. Olivier, G. Gleizes, and P. Barbey (2007), The Hospitalet gneiss dome (Pyrenees) revisited: Lateral flow during Variscan transpression in the middle crust, *Terra Nova*, *19*, 419–453, doi:10.1111/j.1365-3121.2007.00770.x.

Denèle, Y., P. Olivier, G. Gleizes, and P. Barbey (2009), Decoupling between the middle and upper crust during transpression-related lateral flow: Variscan evolution of the Aston gneiss dome (Pyrenees, France), *Tectonophysics, 477*(3–4), 244–261, doi:10.1016/j.tecto.2009.04.033.

Denèle, Y., B. Laumonier, J.-L. Paquette, P. Olivier, G. Gleizes, and P. Barbey (2014), Timing of granite emplacement, crustal flow and gneiss dome formation in the Variscan segment of the Pyrenees, in *The Variscan Orogeny: Extent, Timescale and the Formation of the European Crust*, edited by K. Schulmann et al., *Geol. Soc. London Spec. Publ.*, 405, doi:10.1144/SP405.5.

Destombes, J., J.-C. Guézou, C. Hœpffner, P. Jenny, A. Piqué, and A. Michard (1982), Le Primaire du Massif des Rehamna s.s., problèmes de stratigraphie de séries métamorphiques, in *Le massif Paléozoïque des Rehamna (Maroc): Stratigraphie, Tectonique et Petrogenese d'un segment de la Chaine Varisque, Notes et Mémoires du Service Géologique*, vol. 303, edited by A. Michard, pp. 35–70, Edition du Service géologique du Maroc, Rabat.

Destombes, J., H. Hollard, and S. Willefert (1985), Lower Palaeozoic rocks of Morocco, in *Lower Palaeozoic Rocks of North-Western and West-Central Africa*, edited by C. H. Holland, pp. 91–336, John Wiley, Chichester.

Diot, H. (1989), Mise en place des granitoïdes hercyniens de la Meseta marocaine, Étude structurale des massifs de Sebt de Brikine (Rehamna), de Zaër et d'Oulmès (Massif Central) et d'Aouli-Boumia (Haute Moulouya). Implications géodynamiques, Thèse 3^{e} cycle, 172 pp., Université Paul Sabatier, Toulouse, France.

Diot, H., and J.-L. Bouchez (1991), Structure des massifs granitiques de la Meseta marocaine, marqueurs géodynamiques: Aouli-Bou-Mia (Haute-Moulouya), Zaër (Massif Central) et Sebt de Brikiine (Rehamna), *Geol. Mediterr.*, *18*(1–2), 81–97.

Dodson, M. H. (1973), Closure temperature in cooling geochronological and petrological systems, *Contrib. Mineral. Petrol.*, *40*(3), 259–274, doi:10.1007/BF00373790.

Edel, J.-B., K. Schulmann, E. Skrzypek, and A. Cocherie (2013), Tectonic evolution of the European Variscan belt constrained by palaeomagnetic, structural and anisotropy of magnetic susceptibility data from the Northern Vosges magmatic arc (eastern France), *J. Geol. Soc. London*, *170*, 785–804, doi:10.1144/jgs2011-138.

Edel, J.-B., L. Casini, G. Oggiano, P. Rossi, and K. Schulmann (2014), Early Permian 90° clockwise rotation of the Maures–Estérel–Corsica–Sardinia block confirmed by new palaeomagnetic data and followed by a Triassic 60° clockwise rotation, in *The Variscan Orogeny: Extent, Timescale and the Formation of the European Crust*, edited by K. Schulmann et al., *Geol. Soc. London Spec. Publ.*, *405*, doi:10.1144/SP405.10.

El Hadi, H., A. Tahiri, and A. Reddad (2003), Les granitoïdes hercyniens post-collisionnels du Maroc oriental: Une province magmatique calco-alcaline à shoshonitique, *C. R. Geosci.*, *335*, 959–967, doi:10.1016/j.crte.2003.09.003.

El Hadi, H., J. F. Simancas, A. Tahiri, F. González-Lodeiro, A. Azor, and D. Martínez-Poyatos (2006), Comparative review of the Variscan granitoids of Morocco and Iberia: Proposal of a broad zonation, *Geodinamica Acta*, *19*(2), 103–116, doi:10.3166/ga.19.103-116.

El Kamel, F., and A. El Hassani (2006), Étapes de la structuration et de la sédimentation du bassin viséen de Mechra ben Abbou (Meseta occidentale marocaine), *Geodiversitas*, *28*(4), 529–542.

El Mahi, B., C. Hœpffner, M. Zahraoui, and A. Boushaba (2000a), L'évolution tectono-métamorphique de la zone hercynienne des Rehamna centraux (Maroc), *Bulletin de l'Institut Scientifique Rabat*, *22*(*1999–2000*), 41–57.

El Mahi, B., M. Zahraoui, C. Hœpffner, A. Boushaba, A. Meunier, and D. Beaufort (2000b), Les veines synmétamorphiques de quartz à disthène: Témoins d'un métamorphisme associé à l'amincissement post-orogénique (Meseta occidentale, Maroc), *Pangea*, *33–34*, 27–47.

Engelder, T., and A. Whitaker (2006), Early jointing in coal and black shale: Evidence for an Appalachian-wide stress field as a prelude to the Alleghanian orogeny, *Geology*, *34*(7), 581–584, doi:10.1130/G22367.1

Erraji, A. (1997), Analyse des terrains carbonifères de la region de Jerada (Maroc oriental) à partir des données de terrain, de forage et de sismique réflexion, Thèse 3^{e} cycle, 236 pp., Université de Rabat, Rabat, Morocco.

Essaifi, A., A. Potrel, R. Capdevila, and J.-L. Lagarde (2003), Datation U – Pb : Âge de mise en place du magmatisme bimodal des Jebilet centrales (chaîne Varisque, Maroc) Implications géodynamiques, *C. R. Geosci.*, *335*(2), 193–203, doi:10.1016/S1631-0713(03)00030-0.

Essaifi, A., S. Samson, and K. Goodenough (2014), Geochemical and Sr–Nd isotopic constraints on the petrogenesisand geodynamic significance of the Jebilet magmatism (VariscanBelt, Morocco), *Geol. Mag.*, doi:10.1017/S0016756813000654, in press.

Eusden, J. D., and B. Barreiro (1988), The timing of peak high-grade metamorphism in central-eastern New England, *Maritime Sediments and Atlantic Geology*, *24*(3), 241–255.

Faure, M. (1995), Late orogenic carboniferous extensions in the Variscan French Massif Central, *Tectonophysics*, *14*, 132–153, doi:10.1029/94TC02021.

Faure, M., J.-M. Lardeaux, and P. Ledru (2009), A review of the pre-Permian geology of the Variscan French Massif Central, in *Mechanics of Variscan Orogeny: A Modern View on Orogenic Research*, *C.R. Geosci.*, *341*, edited by K. Schulmann et al., pp. 202–213, Elsevier Science, Paris, doi:10.1016/j.crte.2008.12.001.

Gasquet, D., J. Leterrier, Z. Mrini, and P. Vidal (1992), Petrogenesis of the Hercynian Tichka plutonic complex (Western High Atlas, Morocco): Trace element and Rb–Sr and Sm–Nd isotopic constraints, *Earth Planet. Sci. Lett.*, *108*, 29–44, doi:10.1016/0012-821X(92)90058-4.

Gasquet, D., J.-M. Stussi, and H. Nachit (1996), Les granitoides hercyniens du Maroc dans le cadre de l'evolution geodynamique regionale, *Bull. Soc. Geol. Fr.*, *167*(4), 517–528.

Ghienne, J. F., K. Boumendjel, F. Paris, B. Videt, P. Racheboeuf, and H. A. Salem (2007), The Cambrian-Ordovician succession in the Ougarta Range (western Algeria, North Africa) and interference of the Late Ordovician glaciation on the development of the Lower Palaeozoic transgression on northern Gondwana, *Bull. Geosci.*, *82*(3), 183–214, doi:10.3140/bull.geosci.2007.03.183.

Goldsmith, R. (1988), Tectonic significance of dikes of Westerly Granite, southeastern Connecticut and southwestern Rhode Island, *Northeast. Geol.*, *10*(3), 195–201.

González, F., C. Moreno, and G. Playford (2011), The Gondwana–Laurussia convergence process: Evidence from the Middle Mississippian (Viséan) palynostratigraphic record, *Geol. Mag.*, *148*(2), 317–328, doi:10.1017/S0016756810000713.

Guézou, J.-C., and A. Michard (1976), Note sur la structure du môle côtier mésétien dans l'ouest des Rehamna (Maroc hercynien), *Sciences Géologiques, Bulletin Strasbourg*, *29*(3), 171–182.

Gutiérrez-Alonso, G., J. Fernández-Suárez, T. E. Jeffries, S. T. Johnston, D. Pastor-Galán, J. B. Murphy, M. P. Franco, and J. C. Gonzalo (2011), Diachronous post-orogenic magmatism within a developing orocline in Iberia, European Variscides, *Tectonics*, *30*, TC5008, doi:10.1029/2010TC002845.

Gutiérrez-Alonso, G., S. T. Johnston, A. B. Weil, D. Pastor-Galán, and J. Fernández-Suárez (2012), Buckling an orogen: The Cantabrian Orocline, *GSA Today*, *22*(7), 4–9, doi: 10.1130/GSATG141A.1.

Hatcher, R. D. (2002), Alleghanian (Appalachian) orogeny, a product of zipper tectonics: Rotational transpressive continent-continent collision and closing of ancient oceans along irregular margins, in *Variscan-Appalachian Dynamics: The Building of the Late Paleozoic Basement*, edited by J. R. Martinez Catalán et al., *Geol. Soc. Am. Spec. Pap.*, *364*, 199–208, doi:10.1130/0-8137-2364-7.199.

Hatcher, R. D. (2010), The Appalachian orogen: A brief summary, in *From Rodinia to Pangea: The Lithotectonic Record of the Appalachian Region*, edited by R. P. Tollo et al., *Mem. Geol. Soc. Am.*, *206*, 1–19, doi:10.1130/2010.1206(01).

Hatcher, R. D., B. R. Bream, and A. J. Merschat (2007), Tectonic map of the southern and central Appalachians: A tale of three orogens and a complete Wilson cycle, in *4-D Framework of Continental Crust*, edited by R. D. Hatcher et al., *Mem. Geol. Soc. Am.*, *200*, 595–632, doi:10.1130/2007.1200(29).

Heatherington, A. L., P. A. Mueller, and J. L. Wooden (2010), Alleghanian plutonism in the Suwannee terrane, USA: Implications for late Paleozoic tectonic models, in *From Rodinia to Pangea: The Lithotectonic Record of the Appalachian Region*, edited by R. P. Tollo et al., *Mem. Geol. Soc. Am.*, *206*, 607–620, doi:10.1130/2010.1206(24).

Hermes, O. D. and D. P. Murray (1988), Middle Devonian to Permian plutonism and volcanism in the N American Appalachians, in *The Caledonian-Appalachian Orogen*, vol. 38, edited by A. L. Harrisand and D. J. Fettes, pp. 559–571, Geol. Soc., London, doi:10.1144/GSL.SP.1988.038.01.38.

Hœpffner, C. (1974), Contribution à la géologie structurale des Rehamna (Meseta marocaine méridionale), Le matériel paléozoïque et son évolution hercynienne dans l'est du massif, Thèse 3^{e} cycle, 100 pp., Université Louis Pasteur, Strasbourg, France.

Hœpffner, C. (1987), La tectonique hercynienne dans l'Est du Maroc, Thèse d'État, 280 pp., Université Louis Pasteur, Strasbourg, France.

Hœpffner, C., D. Jeannette, P. Jenny, A. Michard, and A. Piqué (1975a), Relations entre une tectonique de décrochement et un métamorphisme à disthène dans le massif hercynien des Rehamna (Maroc), *Bulletin de la Société Géologique de France, Série 7*, *17*(3), 421–429.

Hœpffner, C., P. Jenny, and A. Piqué (1975b), La tectogenèse hercynienne dans le massif des Rehamna (Maroc). Écaillages et coulissements synmétamorphiques en bordure du môle côtier mésétien, *Sci. Géol., Bull., Strasbourg*, *28*(3), 179–203.

Hœpffner, C., P. Jenny, A. Piqué, and A. Michard (1982), Le métamorphisme hercynien dans le massif des Rehamna, in *Le massif Paléozoïque des Rehamna (Maroc): Stratigraphie, Tectonique et Petrogenese d'un Segment de la Chaine Varisque, Notes et Mémoires du Service Géologique*, vol. 303, edited by A. Michard, pp. 130–149, Editions du Service Géologique du Maroc, Rabat.

Hœpffner, C., A. Soulaimani, and A. Piqué (2005), The Moroccan Hercynides, *J. Afr. Earth Sci.*, *43*(1–3), 144–165, doi:10.1016/j.jafrearsci.2005.09.002.

Hœpffner, C., M. R. Houari, and M. Bouabdelli (2006a), Tectonics of the North African Variscides (Morocco, western Algeria): An outline, *C. R. Geosci.*, *338*(1–2), 25–40, doi:10.1016/j.crte.2005.11.003.

Hœpffner, C., A. Soulaimani, and A. Piqué (2006b), Reply to the Comment on "The Moroccan Hercynides" by Roddaz M., Soula J.-C., Ben Abbou M., Brusset S., Debat P., Ntarmouchant A., Driouch Y, Béziat D., *J. Afr. Earth Sci.*, *45*(4–5), 518–520, doi:10.1016/j.jafrearsci.2006.04.001.

Houari, M.-R., and C. Hœpffner (2003), Late Carboniferous dextral wrench-dominated transpression along the North African craton margin (Eastern High-Atlas, Morocco), *J. Afr. Earth Sci.*, *37*(1–2), 11–24, doi:10.1016/S0899-5362(03)00085-X.

Huon, S., A. Piqué, and N. Clauer (1987), Étude de l'orogenèse hercynienne au Maroc par la datation K-Ar de l'évolution métamorphique de schistes ardoisiers, Study of the Hercynian orogeny in Morocco by the K-Ar isotopic datation of metamorphic evolution in slates, *Sci. Géol., Bull., Strasbourg*, *40*(3), 273–284.

Kharbouch, F., T. Juteau, M. Treuil, J. L. Joron, A. Piqué, and C. Hœpffner (1985), Le volcanisme dinantien de la Meseta marocaine nord-occidentale et orientale; caractères pétrographiques et géochimiques et implications géodynamiques, *Sci. Géol., Bull., Strasbourg*, *38*, 155–163.

Koppers, A. A. P. (2002), ArArCALC – software for ^{40}Ar/^{39}Ar age calculations, *Comput. Geosci.*, *28*(5), 605–619, doi:10.1016/S0098-3004(01)00095-4.

Košuličová, M., and P. Štípská (2007), Variations in the transient prograde geothermal gradient from chloritoid-staurolite equilibria: A case study from the Barrovian and Buchan-type domains in the Bohemian Massif, *J. Metamorph. Geol.*, *25*(1), 19–35, doi:10.1111/j.1525-1314.2006.00674.x.

Kratinová, Z., K. Schulmann, J.-B. Edel, J. Ježek, and U. Schaltegger (2007), Model of successive granite sheet emplacement in transtensional setting: Integrated microstructural and anisotropy of magnetic susceptibility study, *Tectonics*, *26*, TC6003, doi:10.1029/2006TC002035.

Lacquement, F., O. Averbuch, J. L. Mansy, R. Szaniawski, and M. Lewandowski (2005), Transpressional deformations at lateral boundaries of propagating thrust-sheets: The example of the Meuse Valley Recess within the Ardennes Variscan fold-and-thrust belt (N France – S Belgium), *J. Struct. Geol.*, *27*(10), 1788–1802, doi:10.1016/j.jsg.2005.05.017.

Lagarde, J.-L. (1989), Granites tardi carbonifères et déformation crustale. L'exemple de la Méséta marocaine, in *Mémoires et Documents du Centre Armoricain d'étude Structurale des Socles*, vol. 26, 353 pp., Université Rennes I, Rennes, France.

Lagarde, J. -L., and A. Michard (1986), Stretching normal to the regional thrust displacement in a thrust-wrench shear zone, Rehamna Massif, Morocco, *J. Struct. Geol.*, *8*(3–4), 483–492, doi:10.1016/0191-8141(86)90065-9.

Lagarde, J.-L., S. Ait Omar, and B. Roddaz (1990), Structural characteristics of granitic plutons emplaced during weak regional deformation: Examples from late Carboniferous plutons, Morocco, *J. Struct. Geol.*, *12*(7), 805–821, doi:10.1016/0191-8141(90)90056-5.

Le Heron, D. P., J.-F. Ghienne, M. El Houicha, Y. Khoukhi, and J.-L. Rubino (2007), Maximum extent of ice sheets in Morocco during the Late Ordovician glaciation, *Palaeogeogr. Palaeoclimatol. Palaeoecol.*, *245*(1–2), 200–226, doi:10.1016/j.palaeo.2006.02.031.

Marcoux, E., A. Belkabir, H. L. Gibson, D. Lentz, and G. Ruffet (2008), Draa Sfar, Morocco: A Visean (331 Ma) pyrrhotite-rich, polymetallic volcanogenic massive sulphide deposit in a Hercynian sediment-dominant terrane, *Ore Geol. Rev.*, *33*, 307–328, doi:10.1016/j.oregeorev.2007.03.004.

Marhoumi, M. R., C. Hœpffner, J. Doubinger, and R. Rauscher (1983), Données nouvelles sur l'histoire hercynienne de la Meseta orientale au Maroc: l'âge dévonien des schistes de Debdou et du Mekam, *Comptes rendus des séances de l'Académie des sciences, Paris Série II*, *297*(1), 69–72.

Matte, P. (2001), The Variscan collage and orogeny (480–290 Ma) and the tectonic definition of the Armorica microplate: A review, *Terra Nova*, *13*(2), 122–128, doi:10.1046/j.1365-3121.2001.00327.x.

Michard, A. (1967), Plissement concentrique, plissement synschisteux et granitisation dans le Cambro-Ordovicien des Rehamna occidentaux (Maroc), *Compte rendu sommaire des séances de la Société géologique de France*, *8*, 347–348.

Michard, A. (1969), Fractures profondes et décrochements dans les Rehamna (Maroc hercynien), *Compte rendu sommaire des séances de la Société géologique de France*, *3*, 89–90.

Michard, A. (1982), Le massif Paléozoïque des Rehamna (Maroc) : Stratigraphie, Tectonique et Petrogenese d'un segment de la Chaine Varisque, *Notes et Mémoires du Service Géologique, Editions du Service Géologique du Maroc, Rabat*, *303*, 180.

Michard, A., C. Hœpffner, and P. Jenny (1978), Le couloir de cisaillement calédono-hercynien de la Meseta occidentale sur la transversale de Mechra-Ben-Abbou (Rehamna, Maroc) *Bulletin de la Société Géologique de France, Série 7*, *20*(6), 889–894.

Michard, A., C. Hœpffner, A. Soulaimani, and L. Baidder (2008), The Variscan Belt, in *Continental Evolution: The Geology of Morocco, Lecture Notes in Earth Sciences*, vol. 116, edited by A. Michard et al., pp. 65–132, Springer Berlin Heidelberg, doi:10.1007/978-3-540-77076-3_3.

Michard, A., H. Ouanaimi, C. Hœpffner, A. Soulaimani, and L. Baidder (2010a), Comment on Tectonic relationships of Southwest Iberia with the allochthons of Northwest Iberia and the Moroccan Variscides by J.F. Simancas et al. [C. R. Geoscience 341 (2009) 103–113], *C. R. Geosci.*, *342*(2), 170–174, doi:10.1016/j.crte.2010.01.008.

Michard, A., A. Soulaimani, C. Hœpffner, H. Ouanaimi, L. Baidder, E. C. Rjimati, and O. Saddiqi (2010b), The south-western branch of the variscan belt: Evidence from Morocco, *Tectonophysics*, *492*, 1–24, doi:10.1016/j.tecto.2010.05.021.

Mrini, Z., A. Rafi, J. L. Duthou, and P. Vidal (1992), Chronologie Rb-Sr des granitoïdes hercyniens du Maroc; conséquences, *Bull. Soc. Geol. Fr.*, *163*(3), 281–291.

Oukemeni, D., J. Bourne, and T. E. Krogh (1995), Géochronologie U-Pb sur zircon du pluton d' Aouli, Haute Moulouya, Maroc, *Bull. Soc. Geol. Fr.*, *166*(1), 15–21.

Piqué, A. (1973), La déformation des conglomérats dans les zones métamorphiques des Rehamna (Meseta marocaine). I Passage de la fracturation au flux plastique, *Sci. Géol., Bull., Strasbourg*, *26*(2–3), 219–244.

Piqué, A. (2003), Evidence for an important extensional event during the Latest Proterozoic and Earliest Paleozoic in Morocco, *C. R. Geosci.*, *335*(12), 865–868, doi:10.1016/j.crte.2003.08.005.

Piqué, A., D. Jeannette, and A. Michard (1980), The Western Meseta Shear Zone, a major and permanent feature of the Hercynian belt in Morocco, *J. Struct. Geol.*, *2*(1–2), 55–61, doi:10.1016/0191-8141(80)90034-6.

Piqué, A., J.-C. Guézou, C. Hœpffner, P. Jenny, D. Jeannette, and A. Michard (1982), Tectonique du massif des Rehamna. Évolution de la déformation dans les zones métamorphiques hercyniennes, in *Le massif Paléozoïque des Rehamna (Maroc): Stratigraphie, Tectonique et Petrogenese d'un Segment de la Chaine Varisque, Notes et Mémoires du Service Géologique*, vol. 303, edited by A. Michard, pp. 86–129, Editions du Service Géologique du Maroc, Rabat.

Playford, G., F. González, C. Moreno, and A. Al Ansari (2008), Palynostratigraphy of the Sarhlef Series (Mississippian), Jebilet Massif, Morocco, *Micropaleontology*, *54*(2), 89–124.

Pouclet, A., H. Ouazzani, and A. Fekkak (2008), The Cambrian volcano-sedimentary formations of the westernmost High Atlas (Morocco): Their place in the geodynamic evolution of the West African Palaeo-Gondwana northern margin, in *The Boundaries of the West African Craton*, edited by N. Ennih and J.-P. Liégeois, *Geol. Soc. London Spec. Publ.*, *297*, 303–327, doi:10.1144/SP297.15.

Rais-Assa, R., J.-J. Cornée, J. Muller, and J. Sougy (1983), Les unités allochtones du massif des Rehamna Maroc hercynien, *Comptes Rendus de l'Académie des Sciences, Paris, Série II*, *296*, 783–786.

Razin, P., T. Baudin, P. Chèvremont, D. Andries, N. A. Youbi, C. Hœpffner, D. Thiéblemont, and E. M. Chihani (2003), Carte géologique du Maroc au 1/50 000, feuille de Jebel Kharrou, Mémoire explicatif, *Notes et Mémoires du Service Géologique, Rabat*, *436*, 1–105.

Ribeiro, A., et al. (2007), Geodynamic evolution of the SW Europe Variscides, *Tectonics*, *26*, TC6009, doi:10.1029/2006TC002058.

Roddaz, M., S. Brusset, J.-C. Soula, D. Béziat, M. Ben Abbou, P. Debat, Y. Driouch, F. Christophoul, A. Ntarmouchant, and J. Déramond (2002), Foreland basin magmatism in the Western Moroccan Meseta and geodynamic inferences, *Tectonics*, *21*(5), 1043, doi:10.1029/2001TC901029.

Roddaz, M., J.-C. Soula, M. B. Abbou, S. Brusset, P. Debat, A. Ntarmouchant, Y. Driouch, and D. Béziat (2006), Comment on "The Moroccan Hercynides" by Hœpffner et al. (Journal of African Earth Sciences, vol. 43, pp. 144–165), *J. Afr. Earth Sci.*, *45*(4–5), 515–517, doi:10.1016/j.jafrearsci.2006.04.001.

Schulmann, K., U. Schaltegger, J. Ježek, A. B. Thompson, and J. B. Edel (2002), Rapid burial and exhumation during orogeny: Thickening and synconvergent exhumation of thermally weakened and thinned crust (Variscan orogen in Western Europe), *Am. J. Sci.*, *302*(10), 856–879, doi: 10.2475/ajs.302.10.856.

Schuster, R., and K. Stüwe (2008), Permian metamorphic event in the Alps, *Geology*, *36*(8), 603–606, doi:10.1130/G24703A.1.

Simancas, J. F., A. Tahiri, A. Azor, F. G. Lodeiro, and D. J. M. Poyatos (2005), The tectonic frame of the Variscan – Alleghanian orogen in Southern Europe and Northern Africa, *Tectonophysics*, *398*, 181–198, doi:10.1016/j.tecto.2005.02.006.

Simancas, J. F., A. Azor, D. Martínez-Poyatos, A. Tahiri, H. El Hadi, F. González-Lodeiro, A. Pérez-Estaún, and R. Carbonell (2009), Tectonic relationships of Southwest Iberia with the allochthons of Northwest Iberia and the Moroccan Variscides, in *Mechanics of Variscan Orogeny: A Modern View on Orogenic Research*, *C.R. Geosci.*, vol. 341, edited by K. Schulmann et al., pp. 103–113, Comptes Rendus Geoscience, Paris, doi:10.1016/j.crte.2008.11.003.

Tahiri, A., J. F. Simancas, A. Azor, J. Galindo-Zaldívar, F. G. Lodeiro, H. El Hadi, D. M. Poyatos, and A. Ruiz-Constán (2007), Emplacement of ellipsoid-shaped (diapiric?) granite: Structural and gravimetric analysis of the Oulmès granite (Variscan Meseta, Morocco), *J. Afr. Earth Sci.*, *48*, 301–313, doi:10.1016/j.jafrearsci.2007.04.005.

Tahiri, A., P. Montero, H. El Hadi, D. Martínez Poyatos, A. Azor, F. Bea, J. F. Simancas, and F. González Lodeiro (2010), Geochronological data on the Rabat – Tiflet granitoids: Their bearing on the tectonics of the Moroccan Variscides, *J. Afr. Earth Sci.*, *57*(1–2), 1–13, doi:10.1016/j.jafrearsci.2009.07.005.

Thompson, A. B., K. Schulmann, J. Ježek, and V. Tolar (2001), Thermally softened continental extensional zones (arcs and rifts) as precursors to thickened orogenic belts, *Tectonophysics*, *332*(1–2), 115–141, doi:10.1016/S0040-1951(00)00252-3.

Tisserant, D. (1977), Les isotopes du strontium et l'histoire hercynienne du Maroc, Étude de quelques massifs atlasiques et mésétiens, Thèse 3^{e} cycle, 103 pp., Université Louis Pasteur, Strasbourg.

van den Eeckhout, B., and H. J. Zwart (1988), Hercynian crustal-scale extensional shear zone in the Pyrenees, *Geology*, *16*(2), 135–138, doi:10.1130/0091-7613(1988)016<0135:HCSESZ>2.3.CO;2.

Walsh, J. G., J. N. Aleinikoff, and P. Wintsh (2007), Origin of the Lyme Dome and implications for the timing of multiple Alleghanian deformational and intrusive events in southern Connecticut, *Am. J. Sci.*, *307*, 168–215, doi:10.2475/01.2007.06.

Weil, A. B., G. Gutiérrez-Alonso, S. T. Johnston, and D. Pastor-Gálan (2013), Kinematic constraints on buckling a lithospheric-scale orocline along the northern margin of Gondwana: A geologic synthesis, *Tectonophysics*, *582*, 25–49, doi:10.1016/j.tecto.2012.10.006.

West, D. P., D. R. Lux, and A. M. Hussey (1988), $^{40}Ar/^{39}Ar$ hornblende ages from southwestern Maine: Evidence for Late Paleozoic metamorphism, *Maritime Sediments and Atlantic Geology*, *24*(3), 225–239.

Wilson, M., E.-R. Neumann, G. R. Davies, M. J. Timmerman, M. Heeremans, and B. T. Larsen (2004), Permo-Carboniferous magmatism and rifting in Europe: Introduction, in *Permo-Carboniferous Magmatism and Rifting in Europe*, edited by M. Wilson et al., *Geol. Soc. London Spec. Publ.*, *223*, 1–10, doi:10.1144/GSL.SP.2004.223.01.01.

Zartman, R. R., and D. Hermes (1987), Archean inheritance in zircon from late Paleozoic granites from the Avalon zone of southeastern New England: An African connection, *Earth Planet. Sci. Lett.*, *82*(3–4), 305–315, doi:10.1016/0012-821X(87)90204-4.